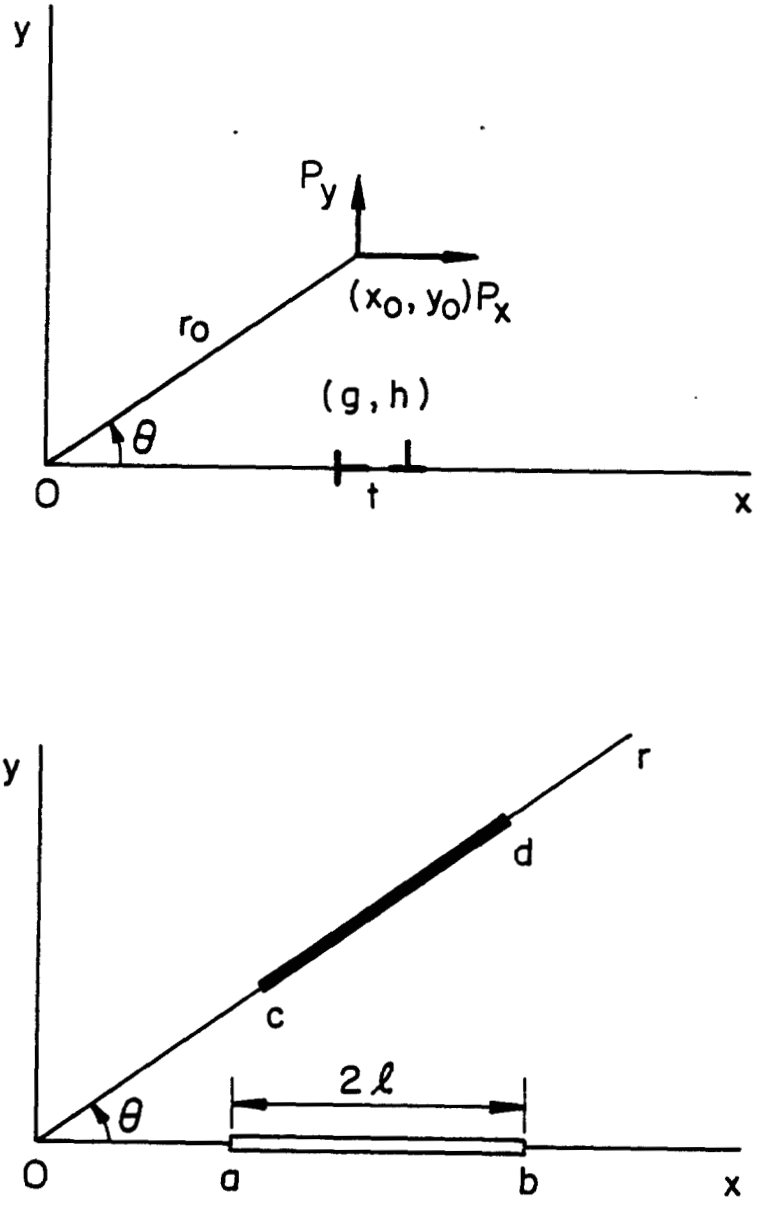

Figure 1. The geometry and notation for the crack-inclusion problem.

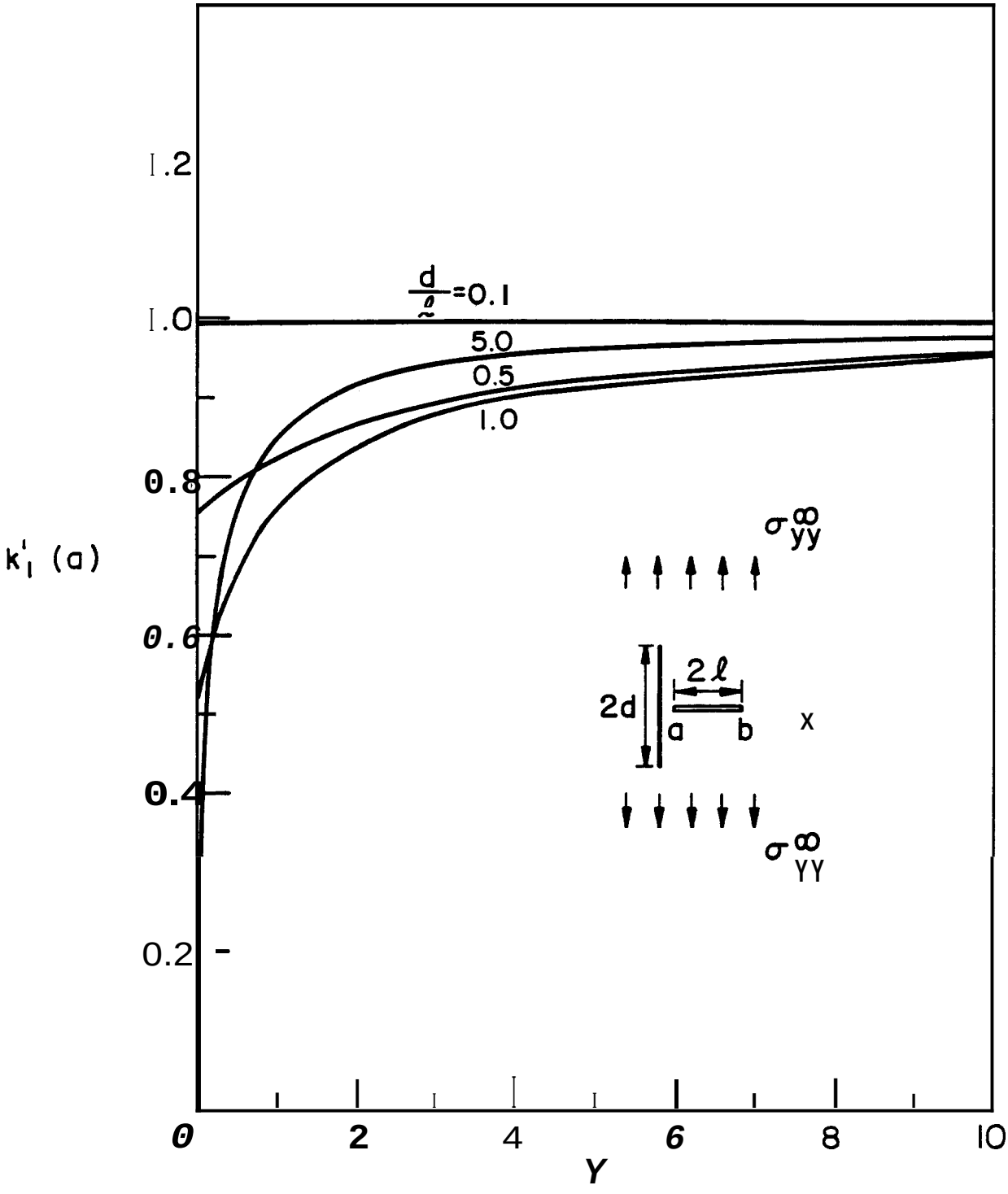

Figure 2. The effect of the stiffness and the relative length of the inclusion on the normalized stress intensity factor $k_1'(a)$; $\sigma^{\infty}_{YY} \neq 0$, $\sigma^{\infty}_{xx} = 0$, $\sigma^{\infty}_{xy} = 0$; $a/a = 0.5$, $\nu = 0.3$.

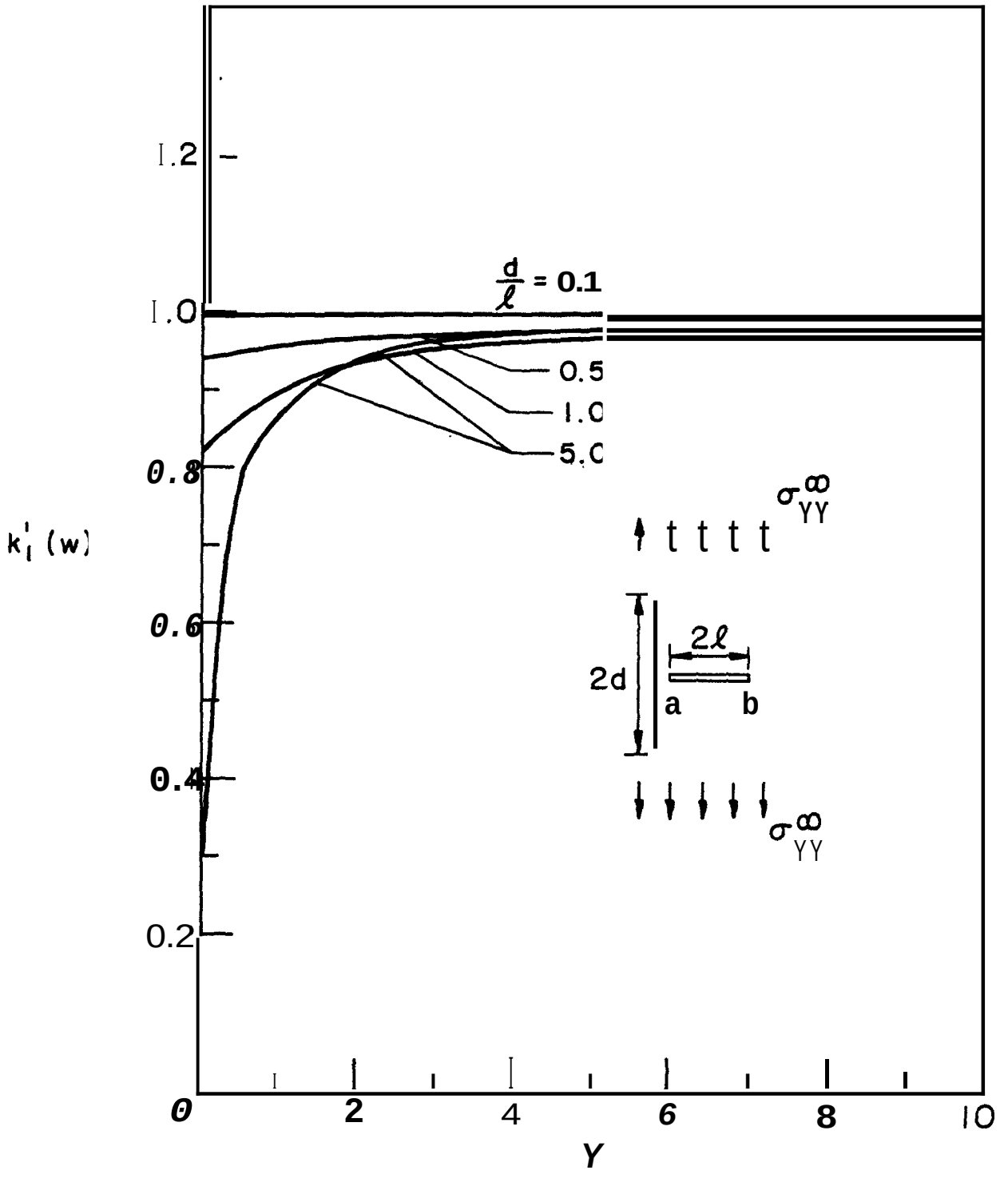

Figure 3. **Normalized stress intensity** factor $k_I'(b)$; $\sigma_{YY}^{\infty} \neq 0$, $\sigma_{XX}^{\infty} = 0 = \sigma_{XY}^{\infty}$, $a/\ell = 0.5$, $\nu = 0.3$,

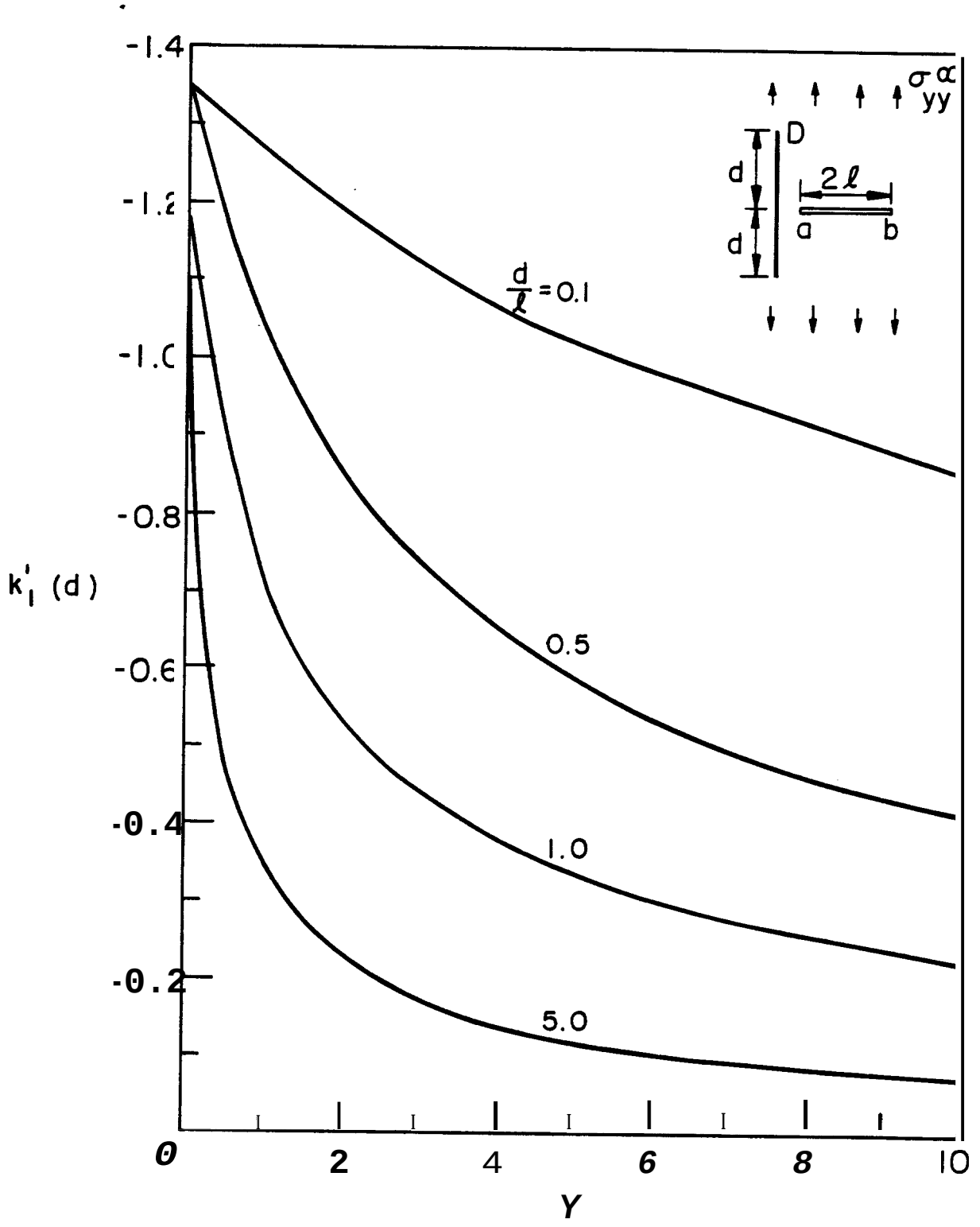

Figure 4. Normalized stress intensity factor at the inclusion end y=d; $\sigma^{\infty}_{YY} \neq 0$, $\sigma^{\infty}_{xx} = \sigma^{\infty}_{xy} = 0$, a/a = 0.5, ν = **0.3.**

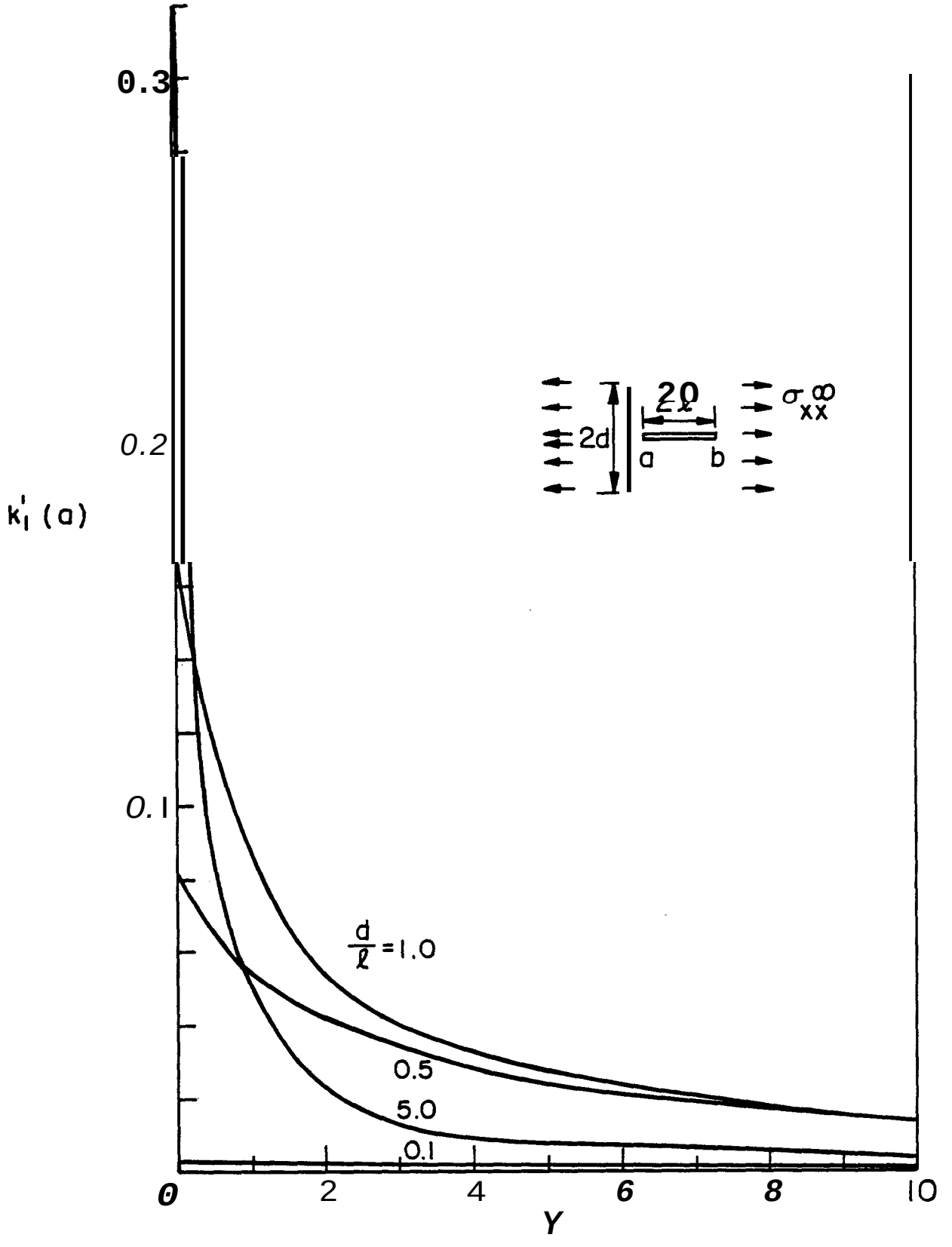

Figure 5. Normalized stress intensity factor at the crack tip x=a; $\sigma_{xx}^{\infty} \neq 0$, $\sigma_{YY}^{\infty} = \sigma_{xy}^{\infty} = 0$, a/a = 0.5, **v = 0.3.**

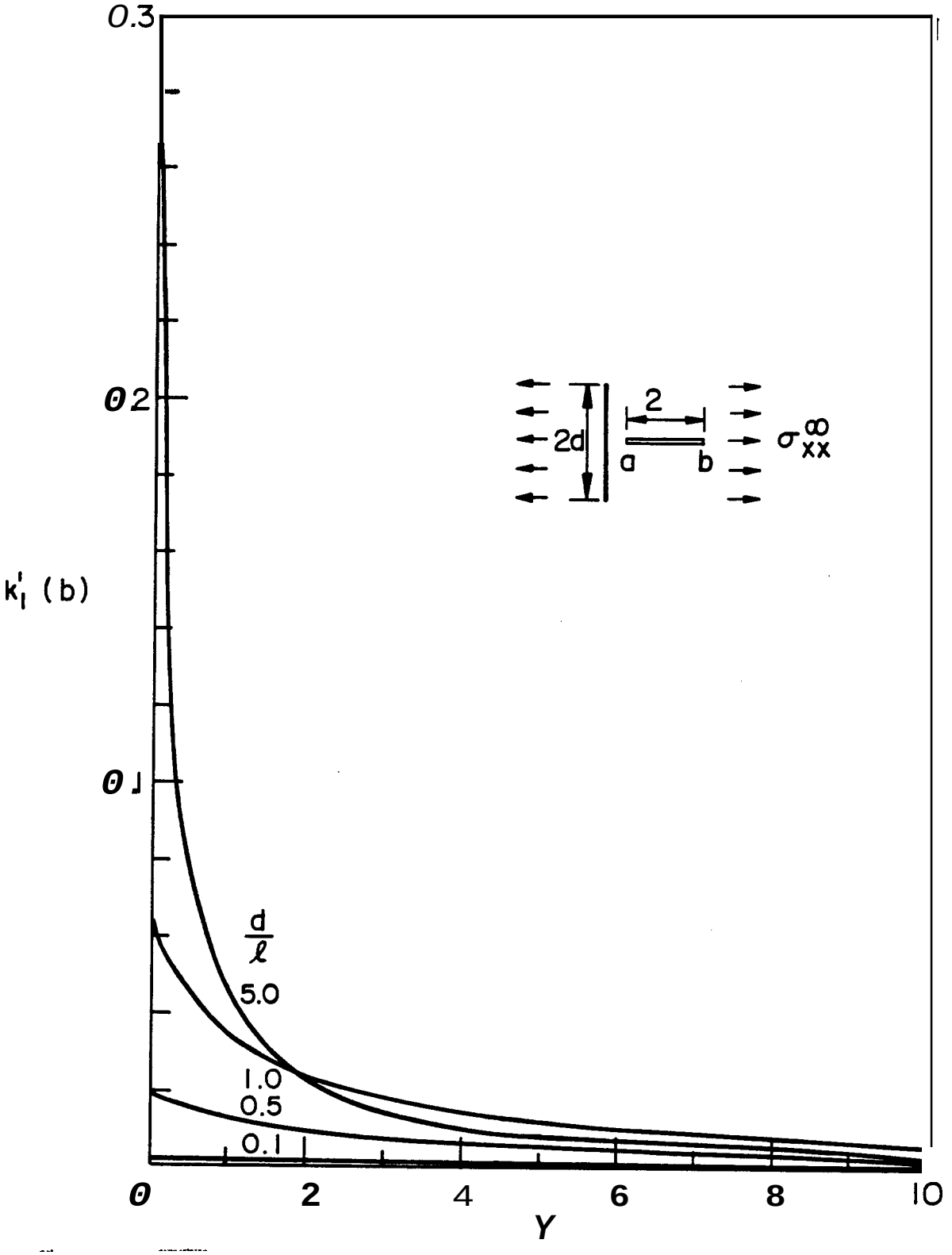

Figure 6. Normalized stress intensity factor at the crack tip x=b; $\sigma_{xx}^{\infty} \neq 0$, $\sigma_{yy} = \sigma_{xy}^{\infty} = 0$, $a/\ell = 0.5$, $\nu = 0.3$.

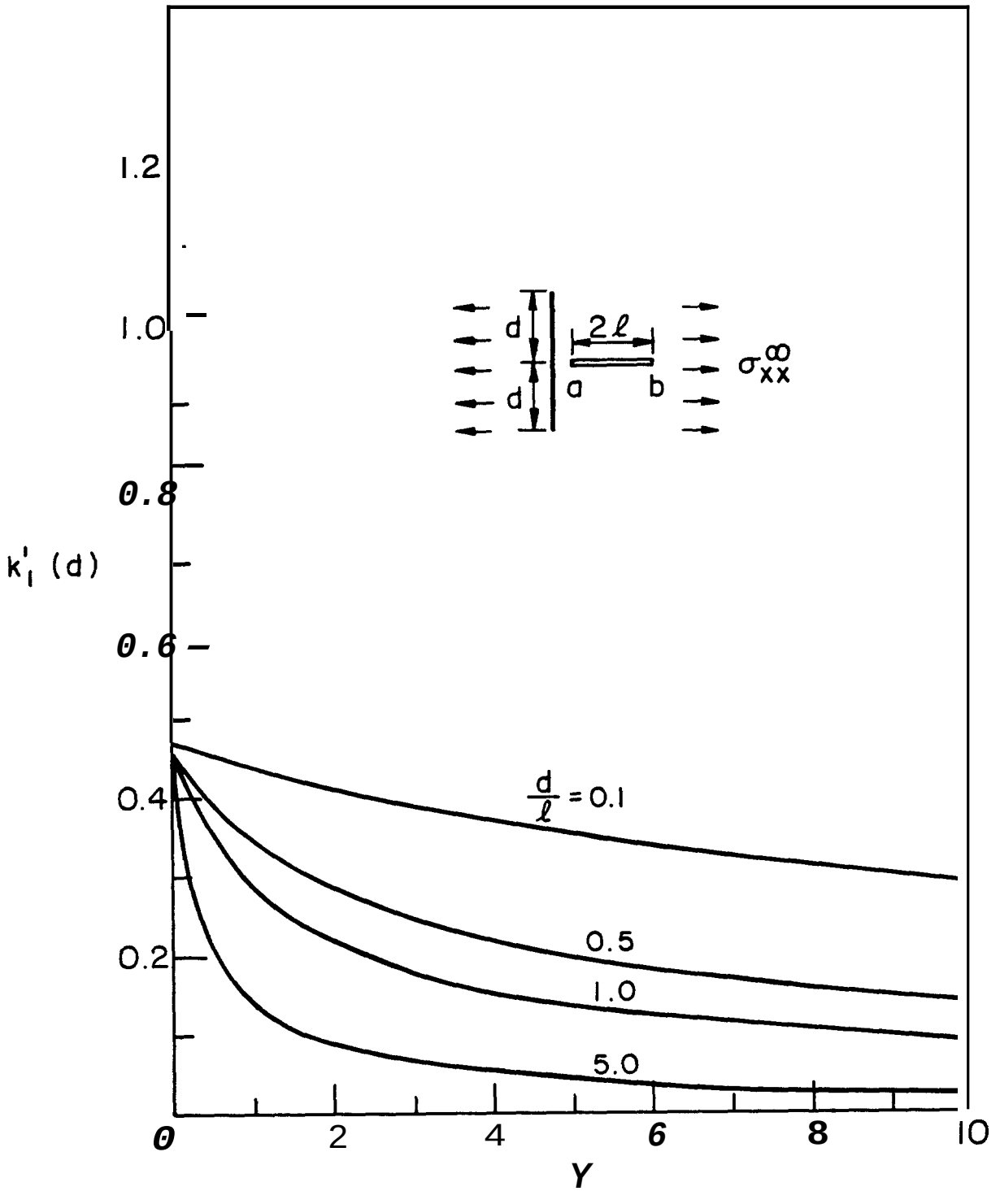

Figure 7. Normalized stress intensity factor at the inclusion end y=d; $\sigma_{xx}^{m} \neq 0$, $\sigma_{yy}^{\infty} = \sigma_{xy}^{\infty} = 0$, a/a = 0.5, v = 0.3.

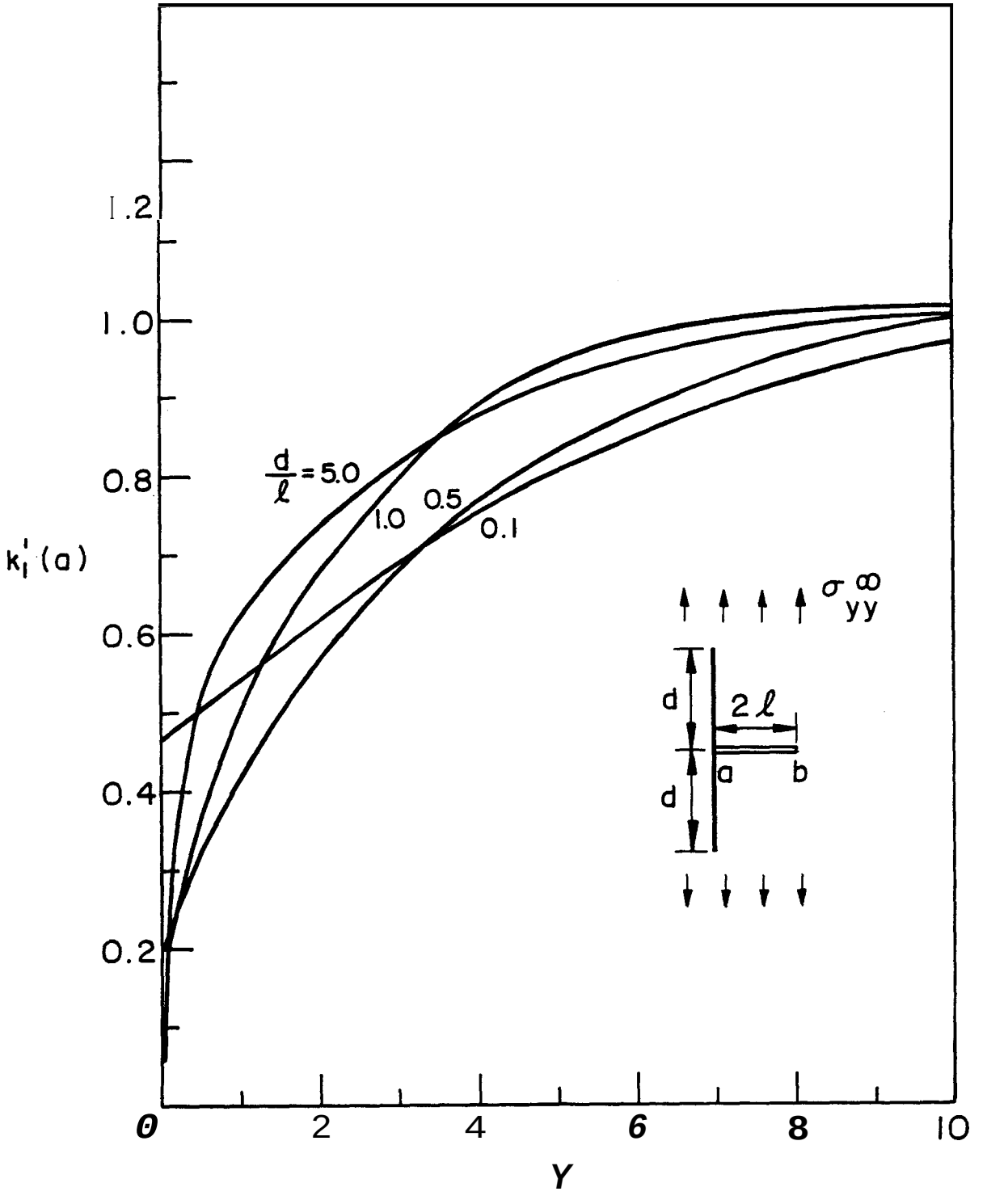

Figure 8. Normalized stress intensity factor at the crack tip x=a=0, $\sigma_{YY}^{\infty} \neq 0$, $\sigma_{xx}^{\infty} = \sigma_{xy}^{\infty} = 0$, v = **0.3.**

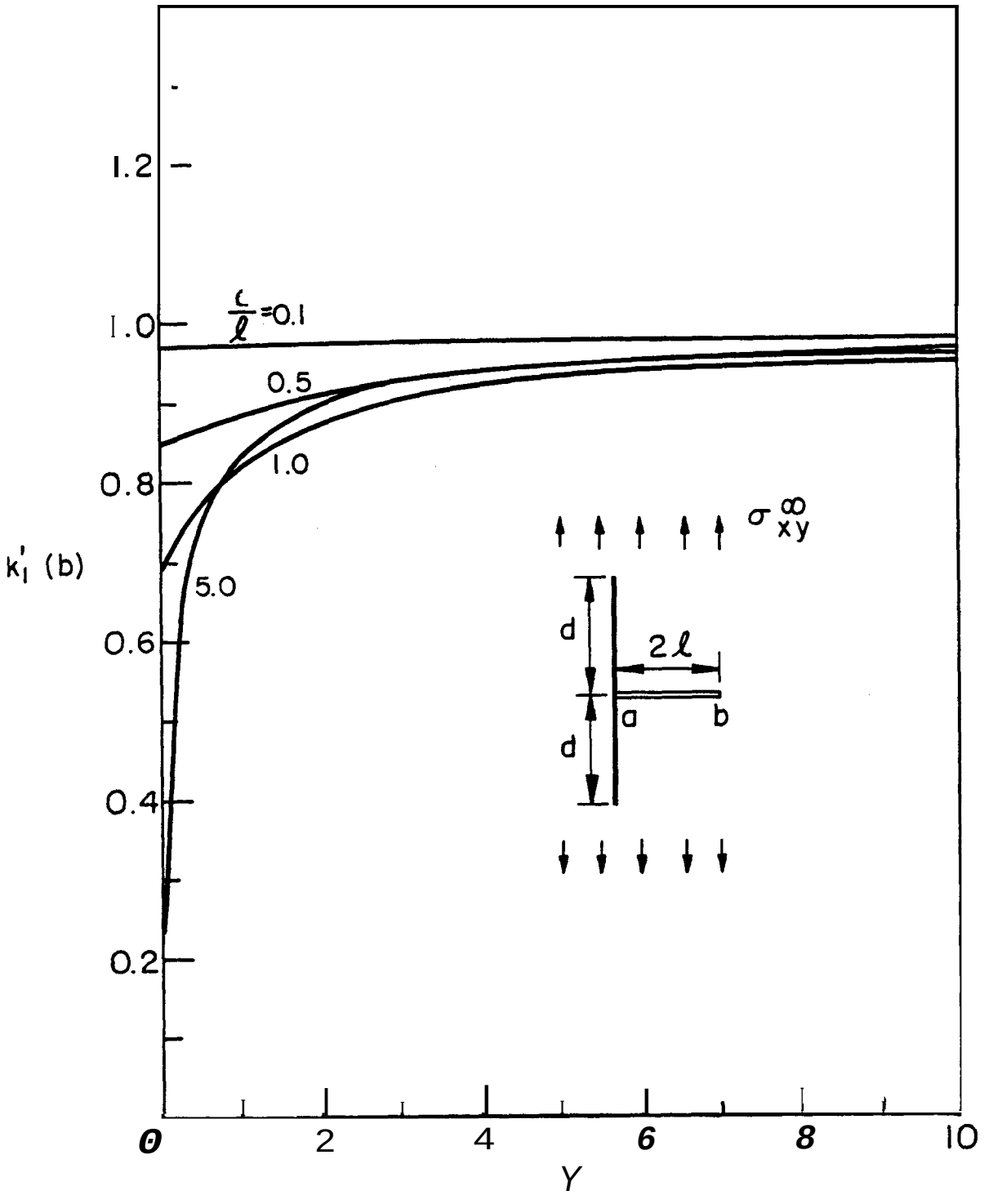

Figure 9. **Normalized stress intensity factor at the crack tip x=b,** $\sigma_{yy}^{\infty} \neq 0$, $\sigma_{xx}^{\infty} = \sigma_{xy}^{\infty} = 0$, **v = 0.3, a = 0.**

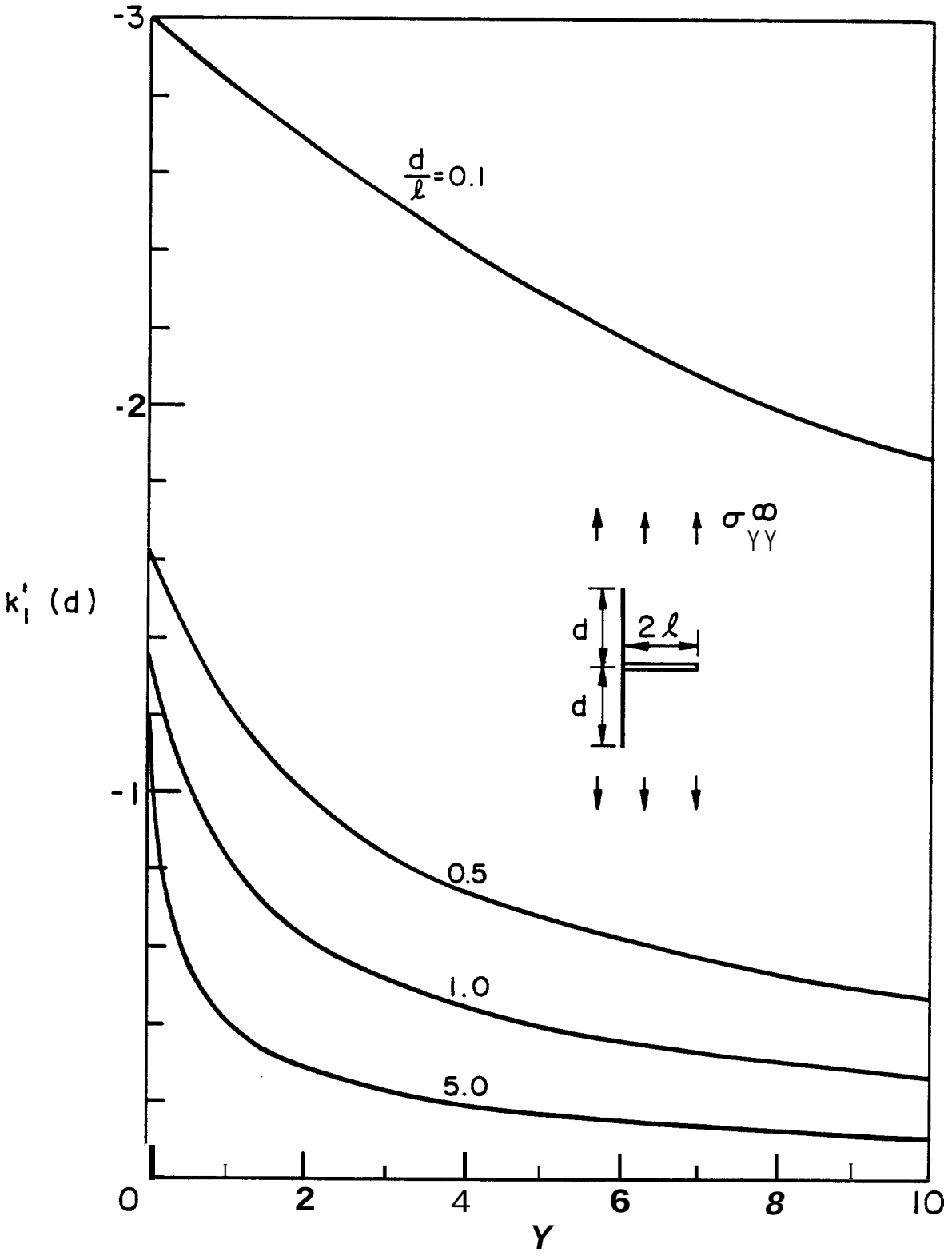

Figure 10. Normalized stress intensity factor at the inclusion end y=d, $\sigma_{yy}^{\infty} \neq 0$, $\sigma_{xx}^{\infty} = \sigma_{xy}^{\infty} = 0$, $\nu = 0.3$, $a = 0$.

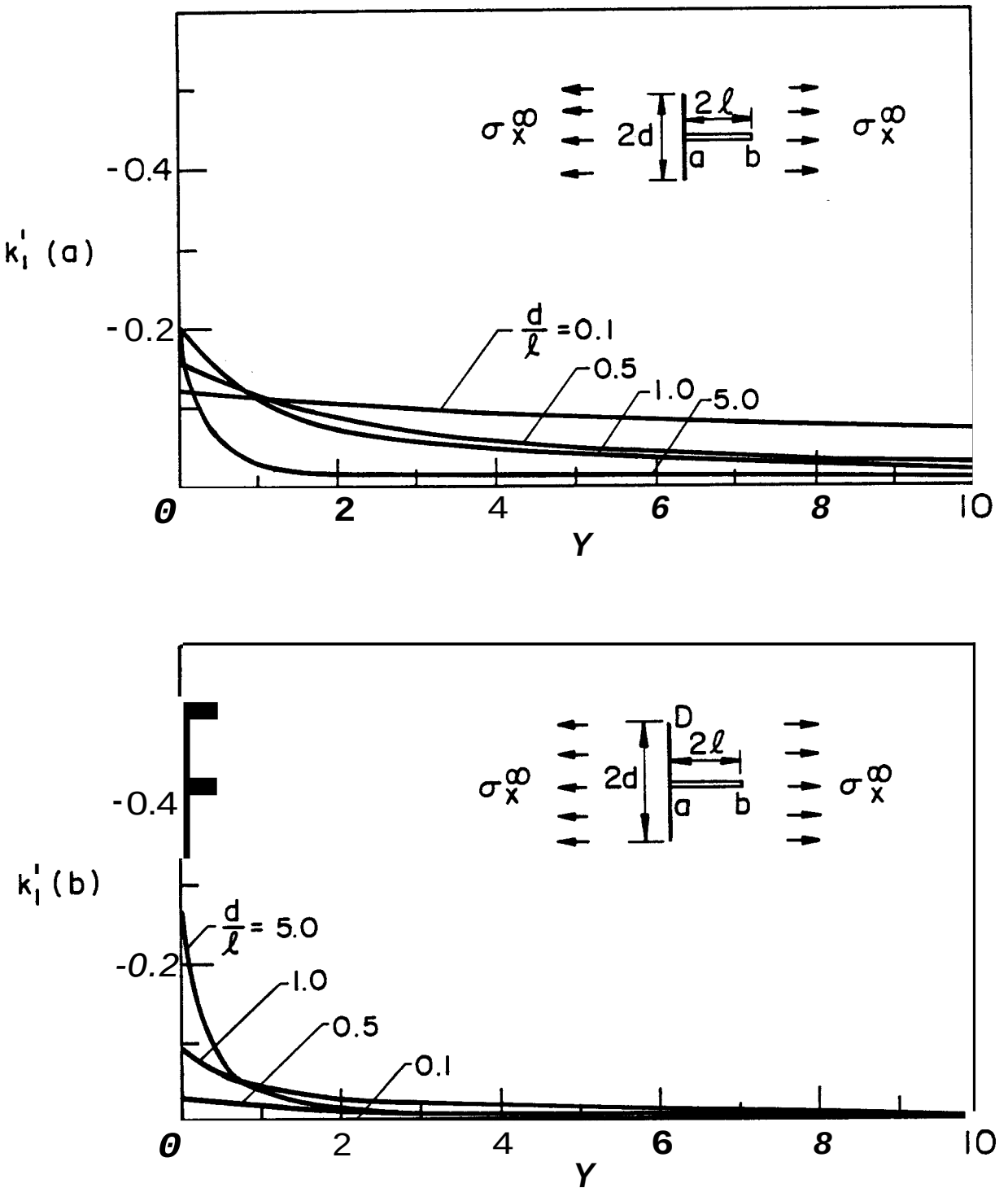

Figure 11. Normalized stress intensity factors at the crack tips x=a=0 and x=b; $\sigma_{xx}^{m} \neq 0$, $\sigma_{YY}^{\infty} = \sigma_{xy}^{\infty} = 0$, a = 0, **v = 0.3.**

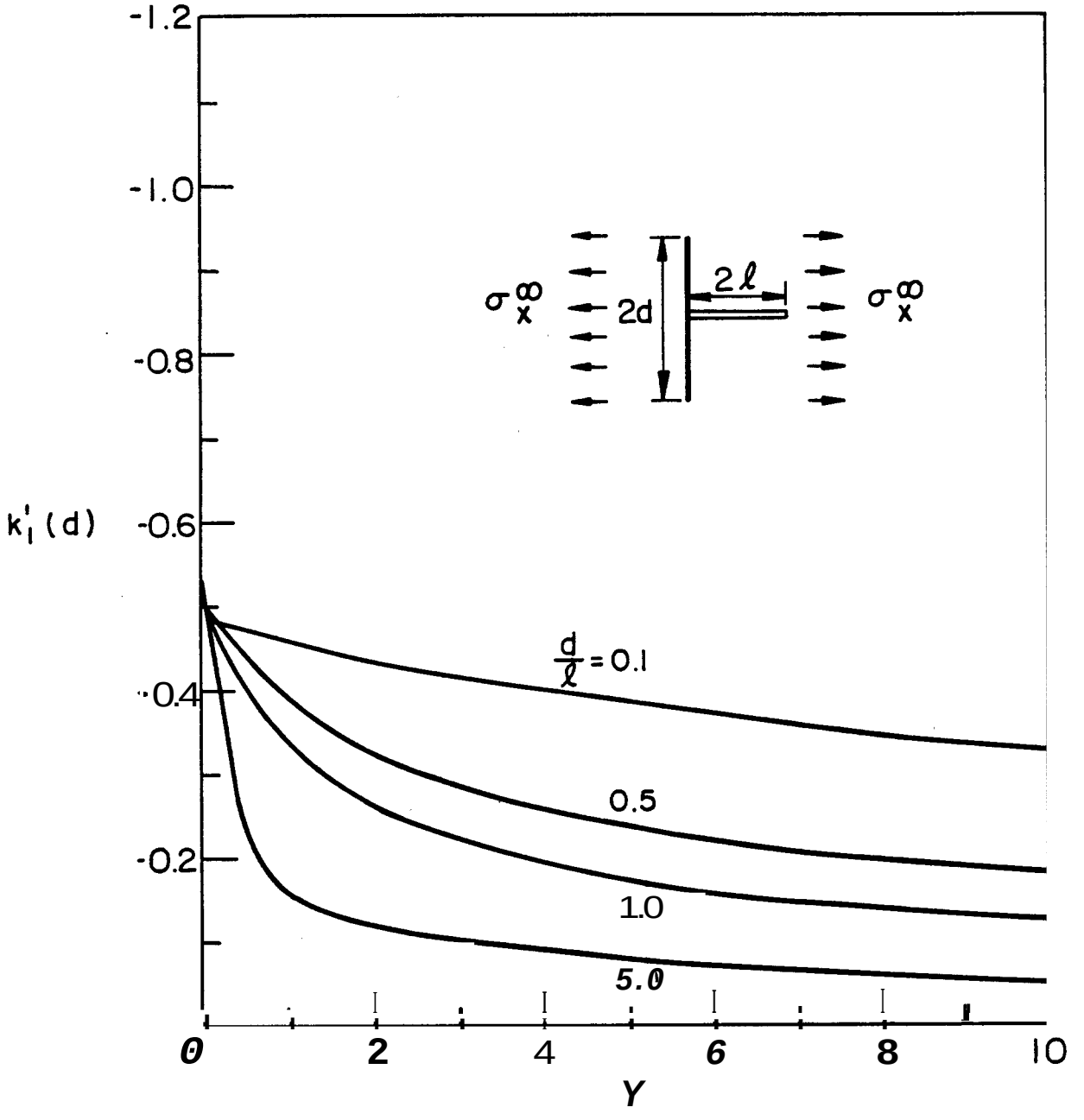

Figure 12. Normalized stress intensity factor at the inclusion end y=d; $\sigma_{xx}^\infty \neq 0$, $\sigma_{YY}^\infty = \sigma_{xy}^\infty = 0$, a = 0, v = 0.3.

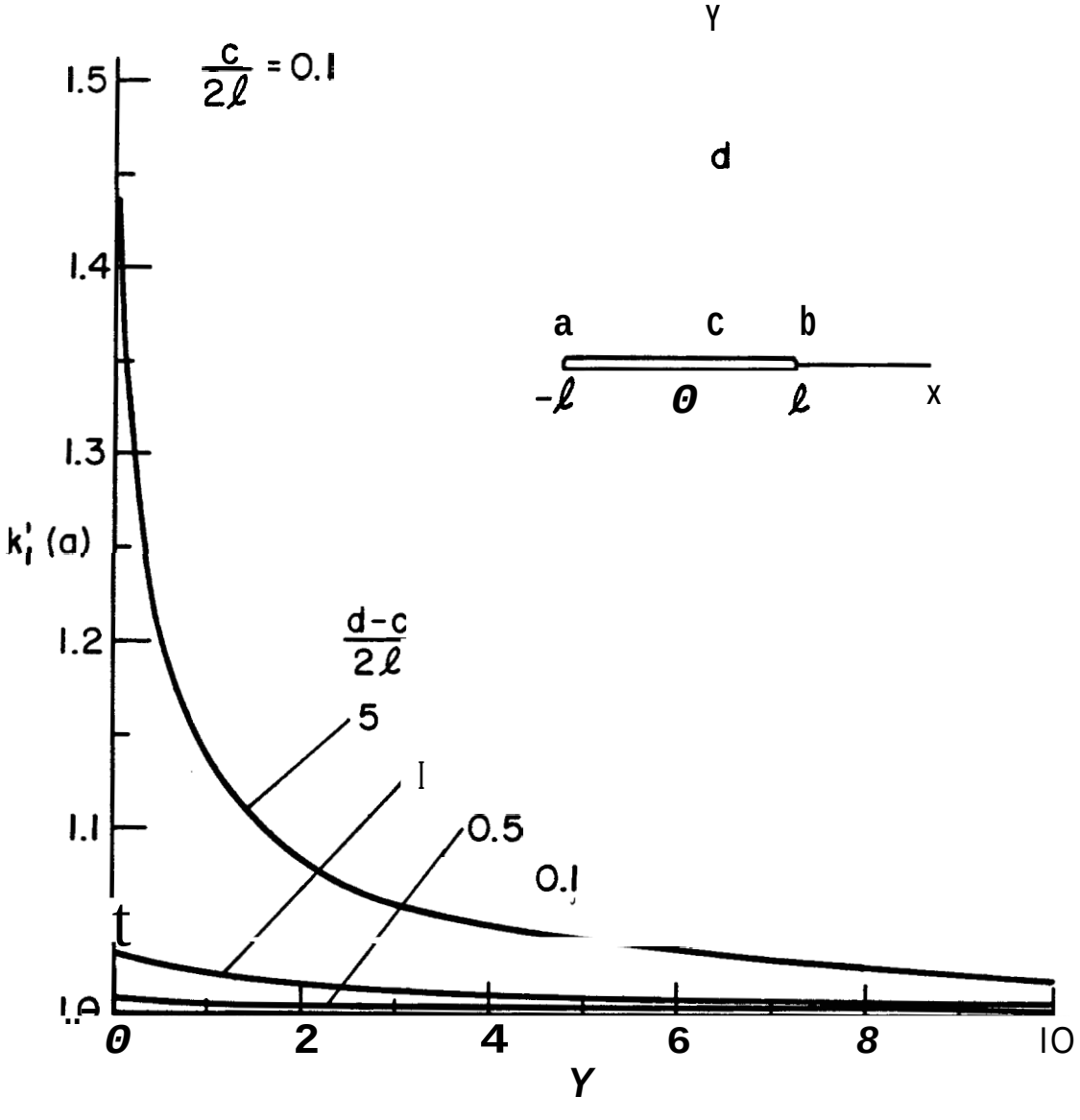

Figure 13. Mode I stress intensity factor at the crack tip $x=a=-\ell$; $\sigma^{\infty}_{yy} \neq 0$, $\sigma^{\infty}_{xx} = 0$, $\sigma^{\infty}_{xy} = 0$, $e = \pi/2$, $c = 0.22$, $b = \ell$, $\nu = 0.3$.

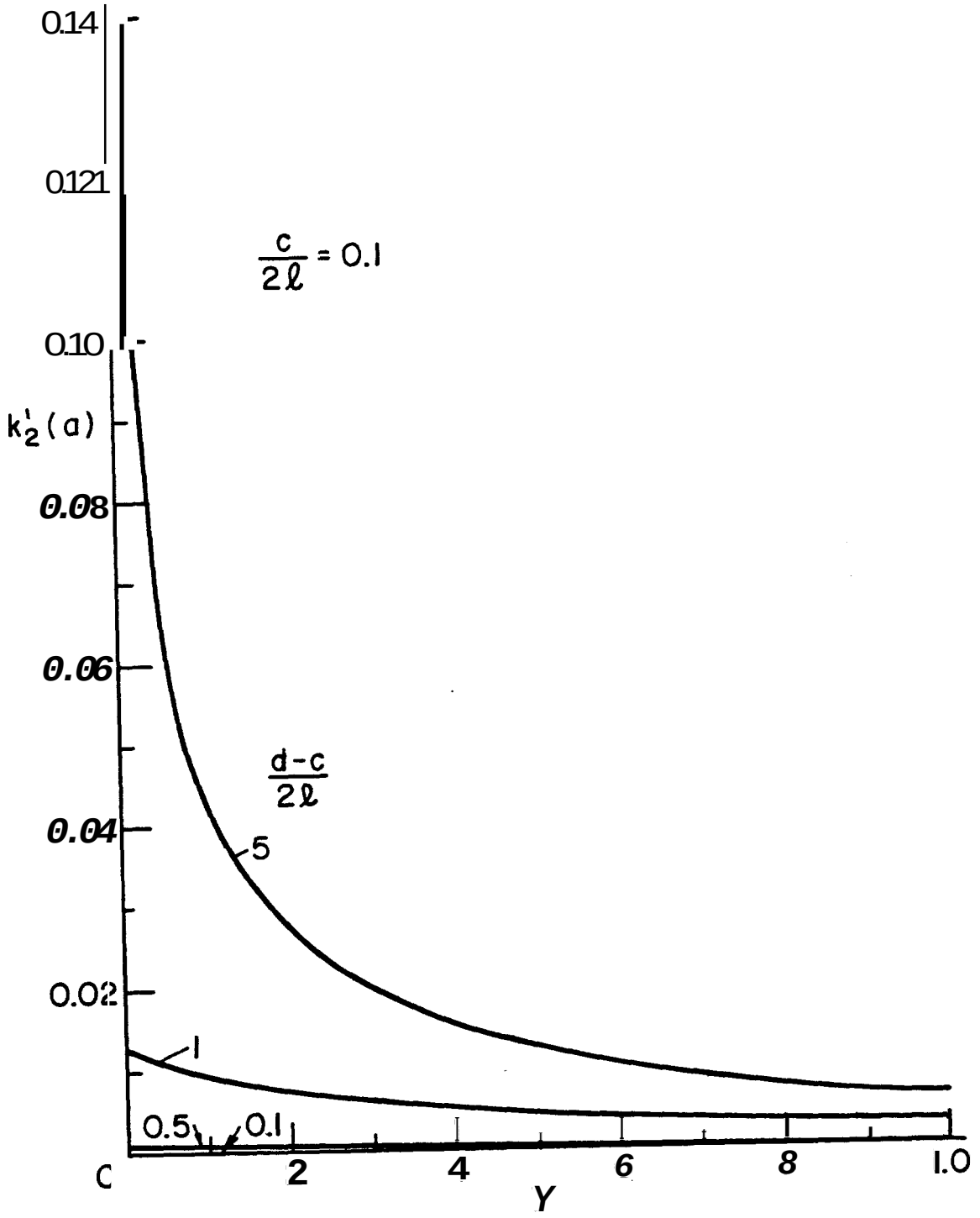

Figure 14. Mode II stress intensity factor at the crack tip x=a=-ℓ; $\sigma_{YY}^{\infty} \neq 0$, $\sigma_{xx}^{\infty} = \sigma_{xy}^{\infty} = 0$, $\theta = \pi/2$, $c = 0.2\ell$, $b = \ell$, $\nu = 0.3$.

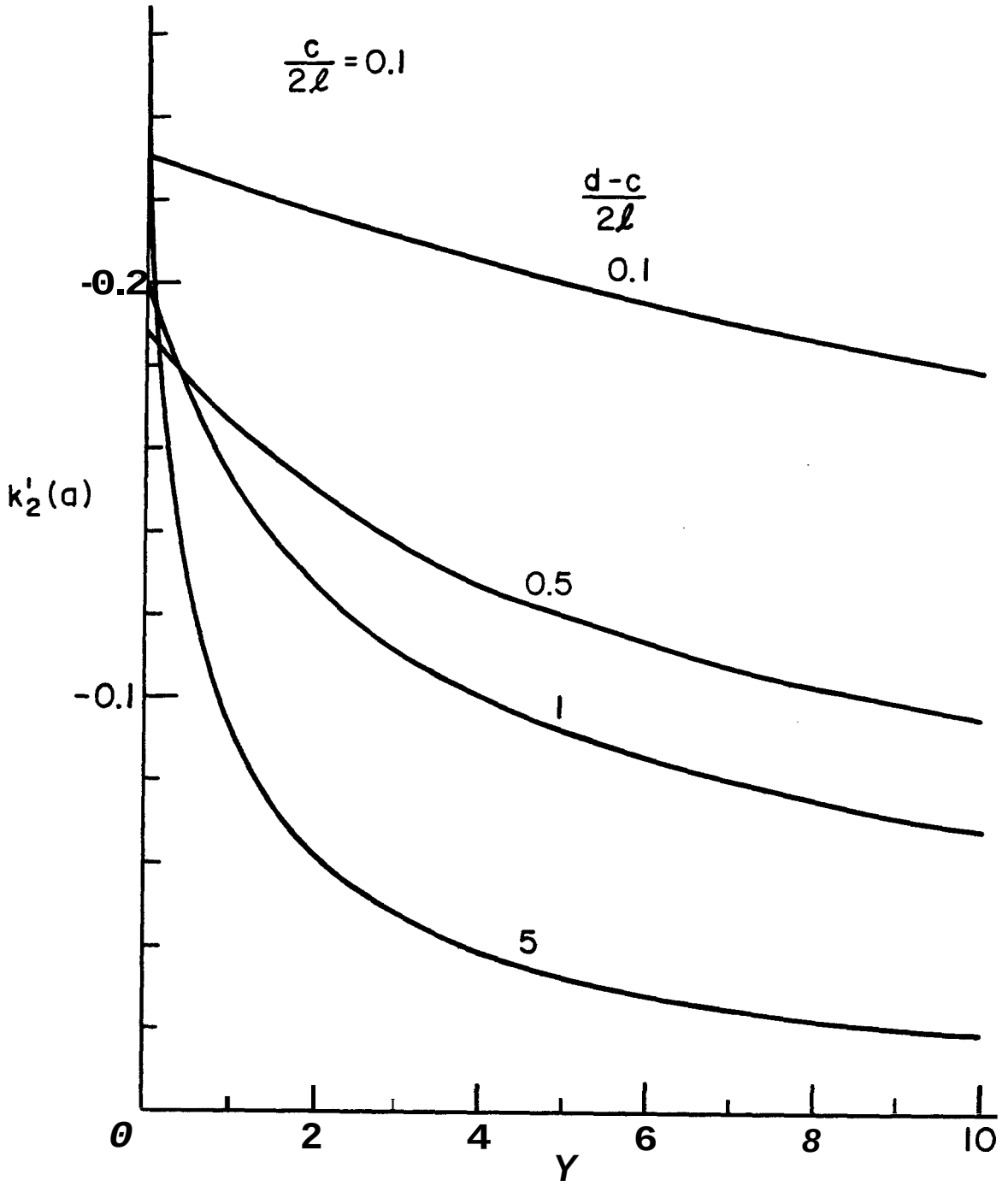

Figure 15. Stress intensity factor at the inclusion end $y=c$; $\sigma^{\infty}_{YY} \neq 0$, $a^{\infty}_{xx} = \sigma^{\infty}_{xy} = 0$, $\theta = \pi/2$, $c = 0.2\ell$, $\nu = 0.3$, $b = \ell$.

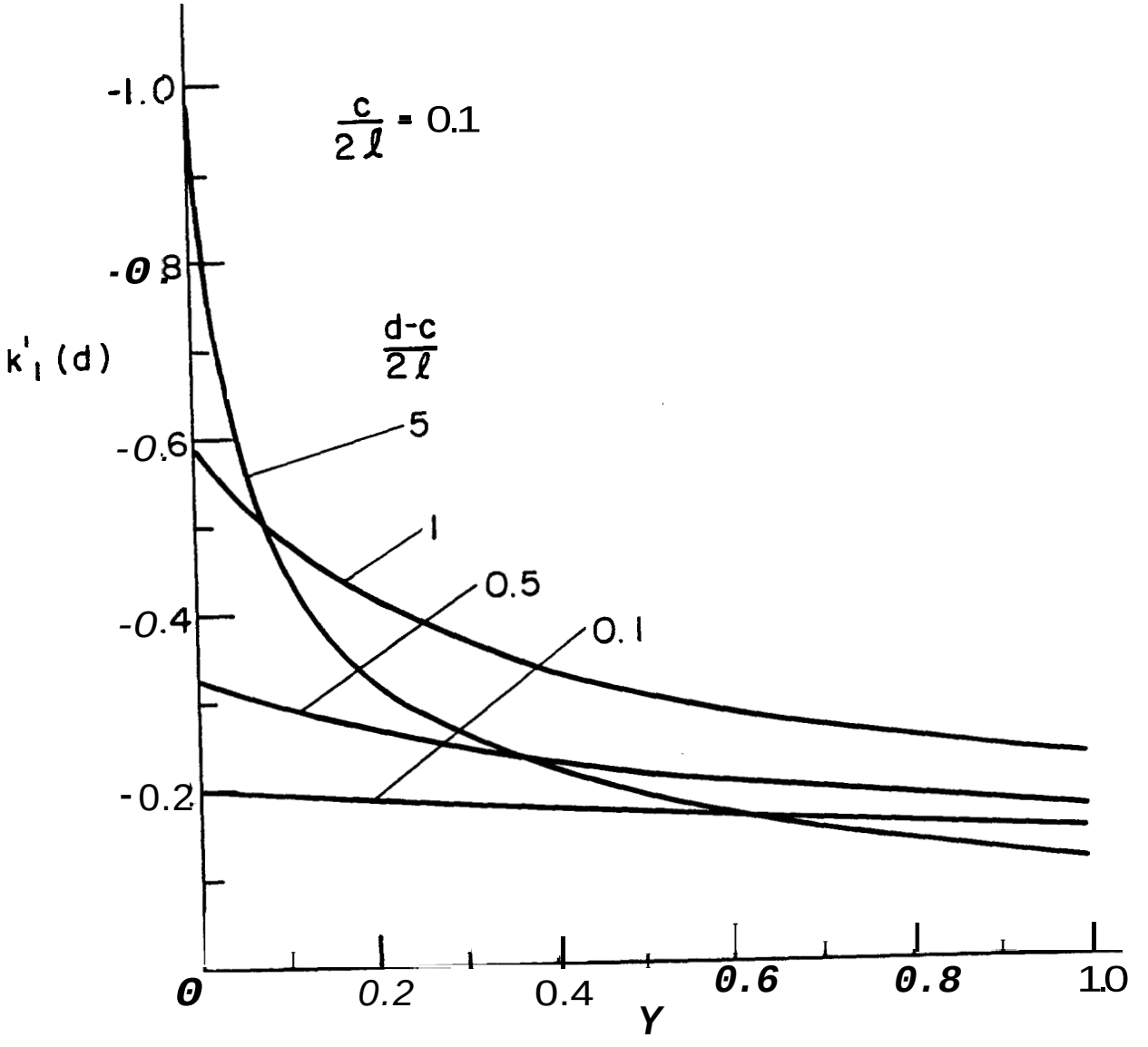

Figure 16. Stress intensity factor at the inclusion end y=d; $\sigma^{\infty}_{yy} \neq 0$, $\sigma^{\infty}_{xx} = \sigma^{\infty}_{xy} = 0$, $\nu = 0.3$, $\theta = \pi/2$, $c = 0.2\ell$, $b = \ell = -a$.

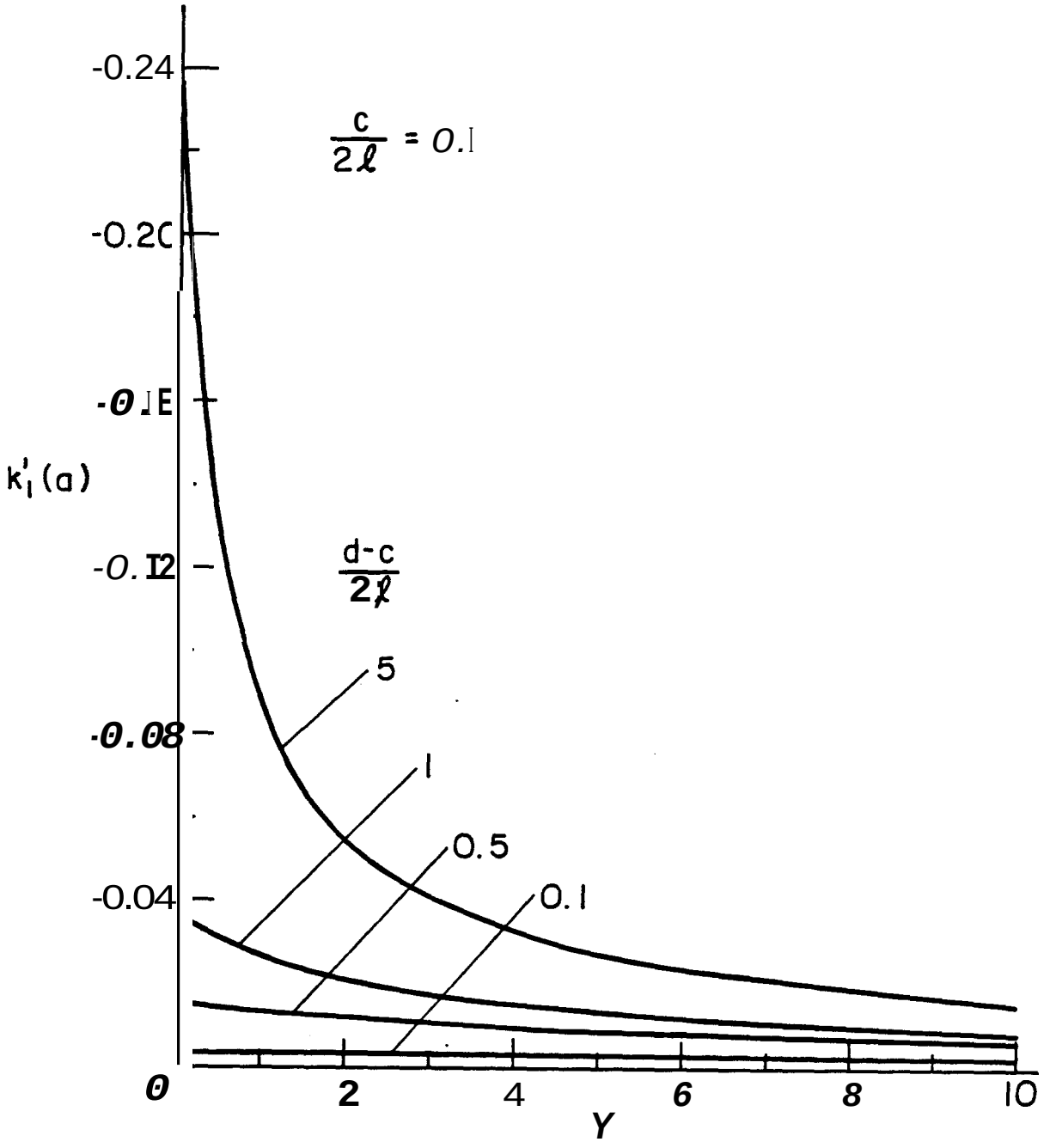

Figure 17. Mode I stress intensity factor at the crack tip $x=a=-\ell$; $\sigma^{\infty}_{xx} \neq 0$, $\sigma^{\infty}_{yy} = \sigma^{\infty}_{xy} = 0$, $\theta = \pi/2$, $\nu = 0.3$, $c = 0.2\ell$, $b = \ell$.

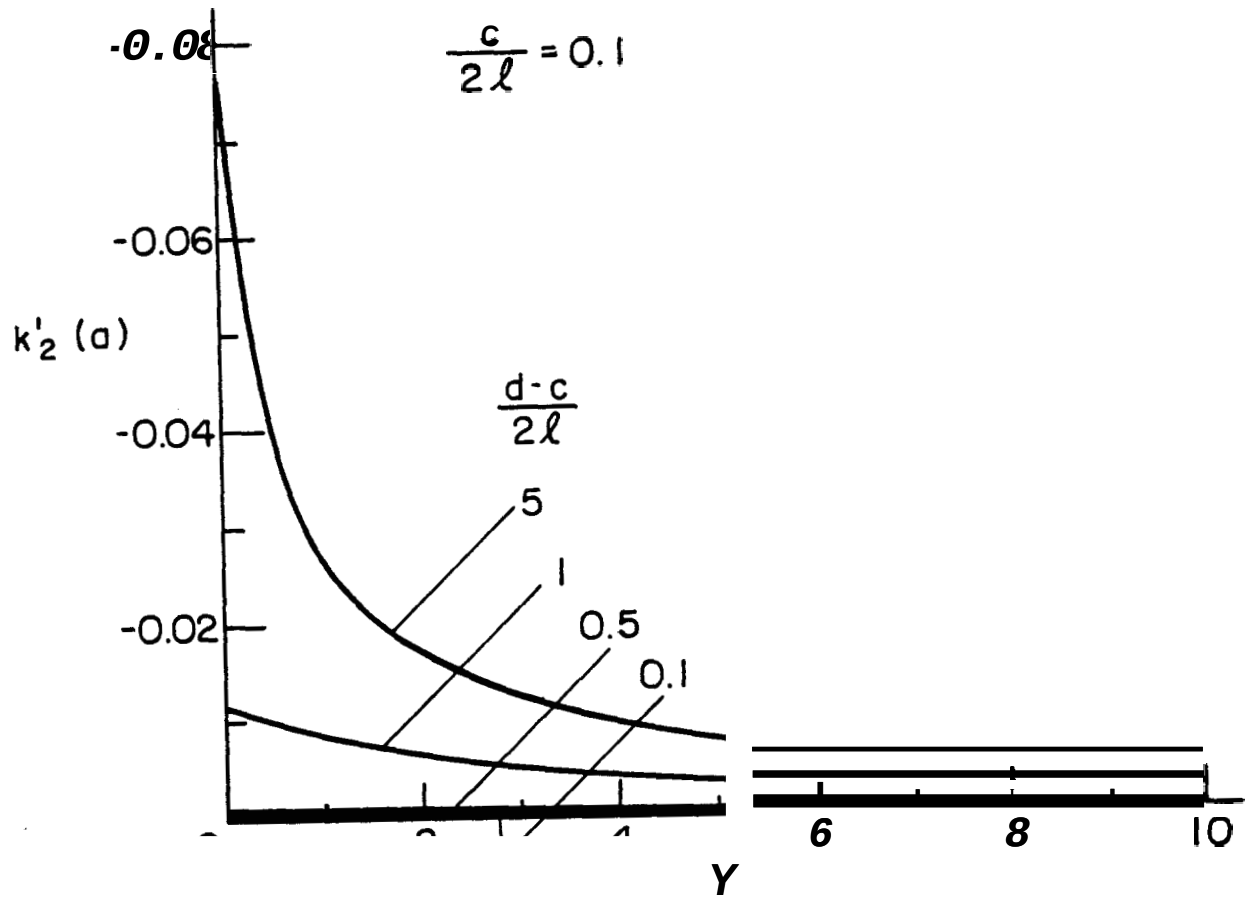

Figure 18. Mode II stress intensity factor at the crack tip $x=a=-\ell$; $\sigma^{\infty}_{xx} \neq 0$, $\sigma^{\infty}_{yy} = \sigma^{\infty}_{xy} = 0$, $\nu = 0.3$, $\theta = \pi/2$, $c = 0.2\ell$, $b = \ell$.

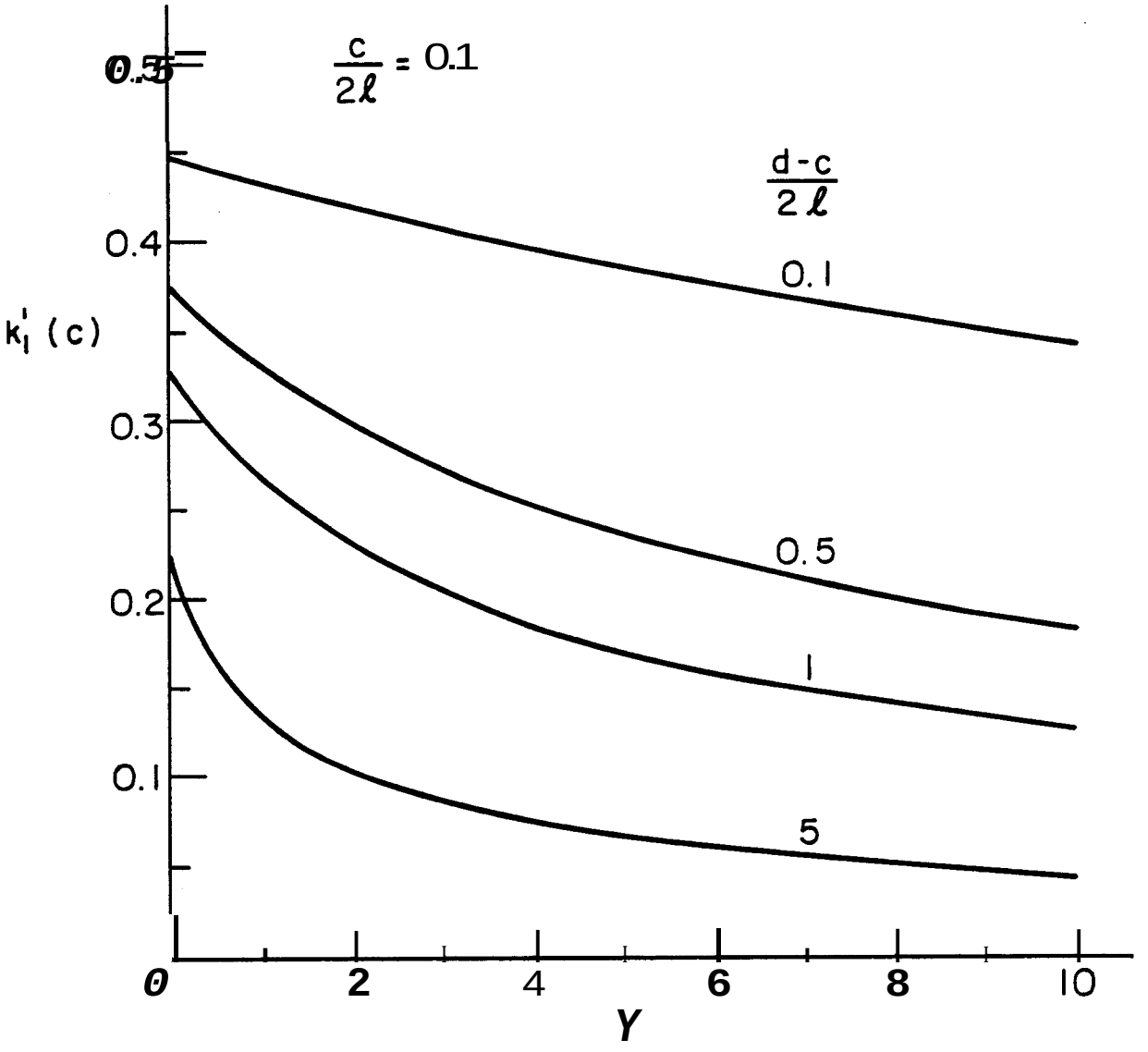

Figure 19. Stress intensity factor at the inclusion end y = c; $\sigma^{\infty}_{xx} \neq 0$, $\sigma^{\infty}_{YY} = \sigma^{\infty}_{xy} = 0$, $\nu = 0.3$, $c = 0.2\ell$, $e = \pi/2$, $b = \ell = -a$.

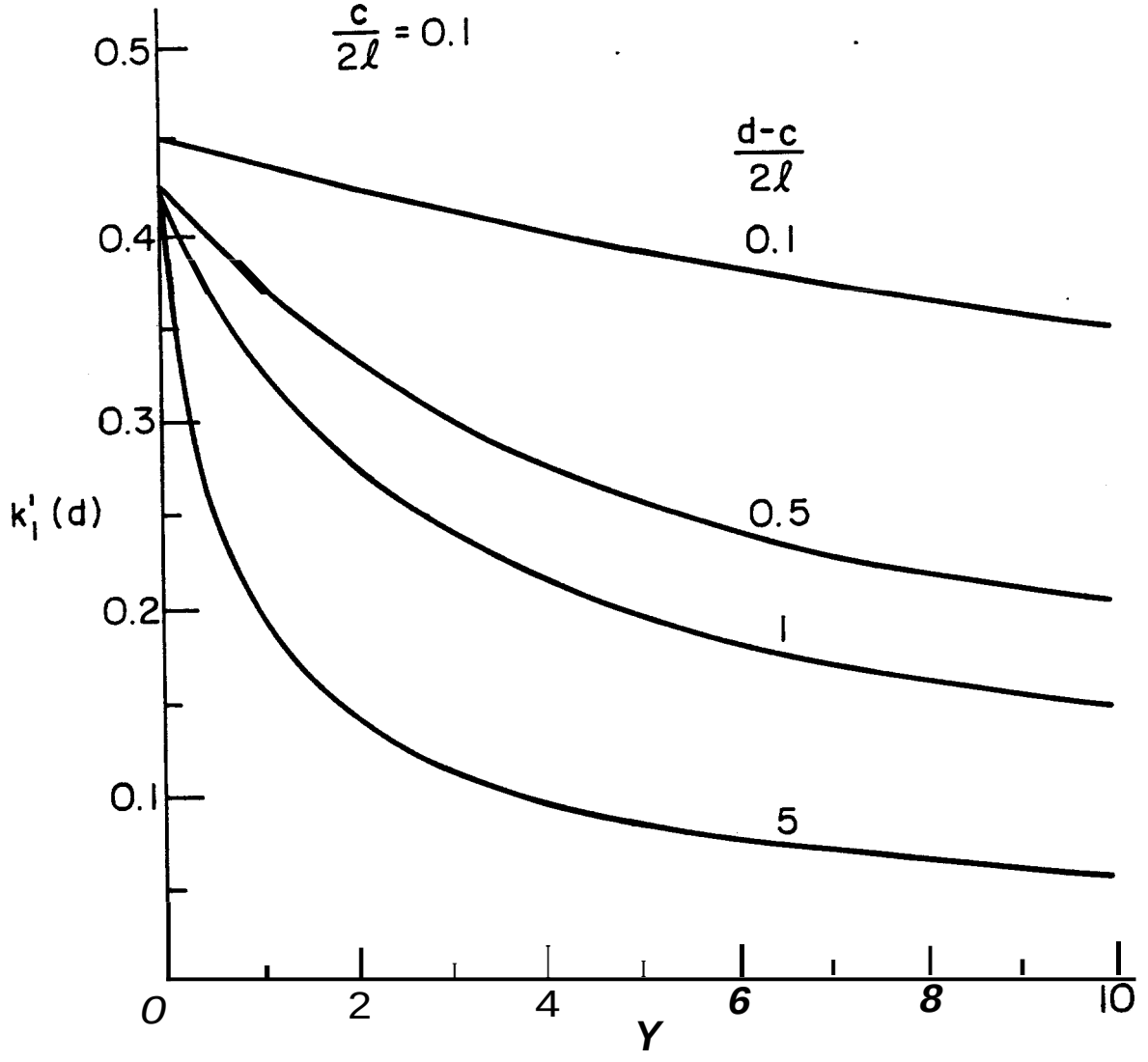

Figure 20. Stress intensity factor at the inclusion end y = d; $\sigma^{\infty}_{xx} \neq 0$, $\sigma^{\infty}_{YY} = \sigma^{\infty}_{xy} = 0$, $\nu = 0.3$, $\theta = \pi/2$, $c = 0.2\ell$, $b = R = -a$.

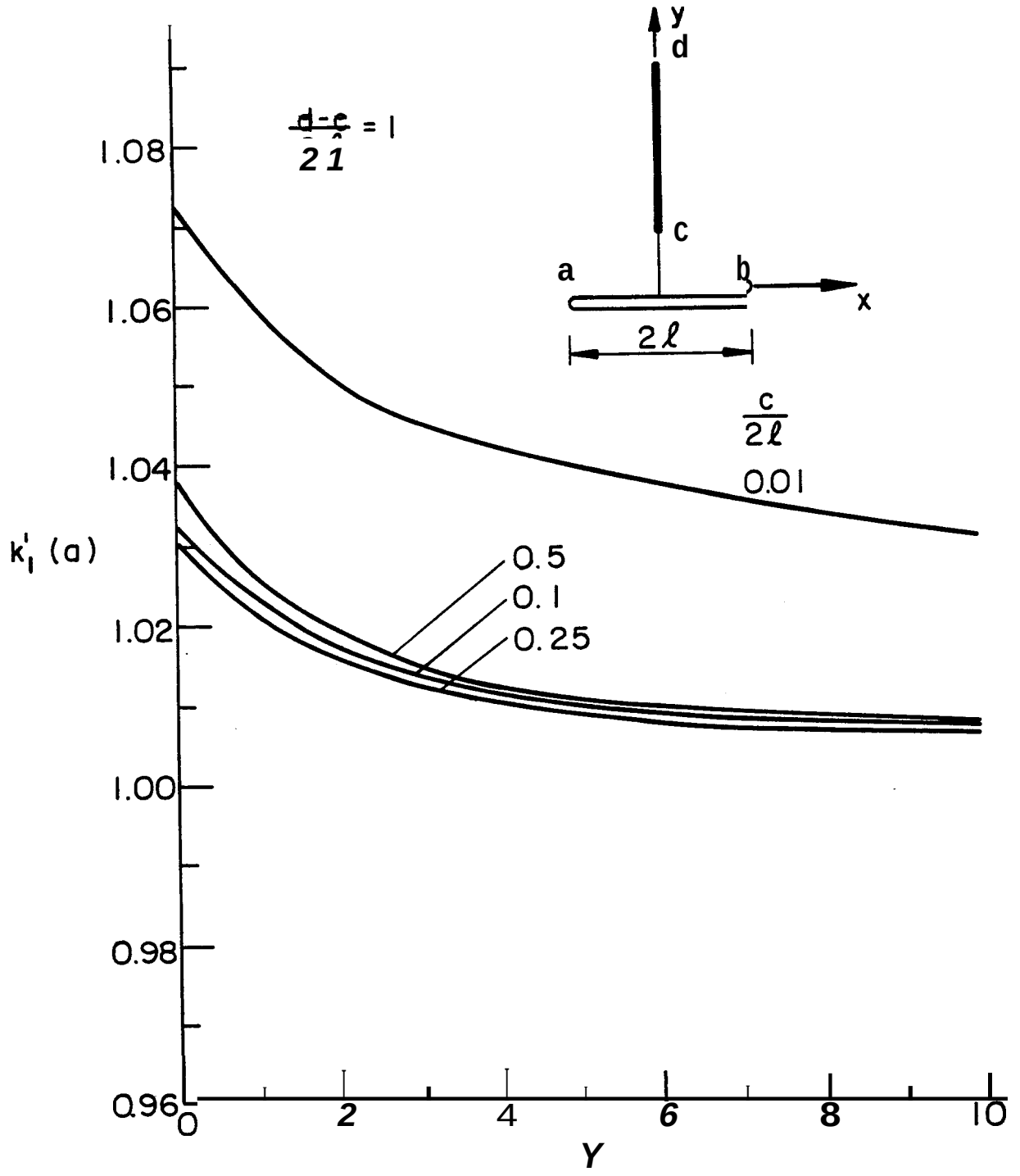

Figure 21. Mode I stress intensity factor at the crack tip $x = a = -\ell$; $\sigma^{\infty}_{YY} \neq 0$, $\sigma^{\infty}_{xx} = \sigma^{\infty}_{xy} = 0$, $\theta = \pi/2$, $\nu = 0.3$, $d-c = 2\ell$, $b = \ell$.

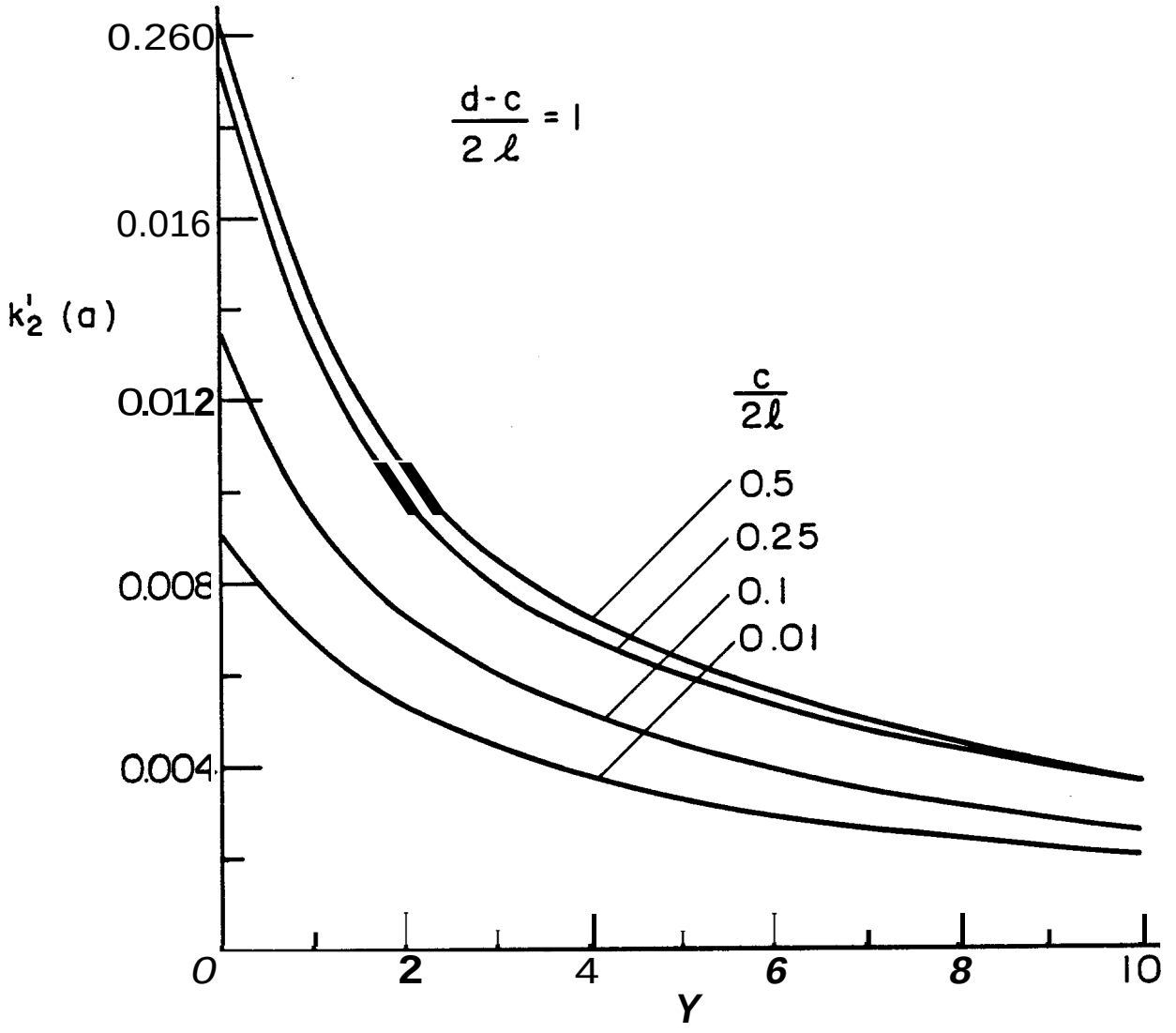

Figure 22. Mode II stress intensity factor at the crack tip $x = a = -\ell$; $\sigma^{\infty}_{YY} \neq 0$, $\sigma^{\infty}_{xx} = \sigma^{\infty}_{xy} = 0$, $\nu = 0.3$, $\theta = \pi/2$, $d-c = 2\ell$, $b = \ell$.

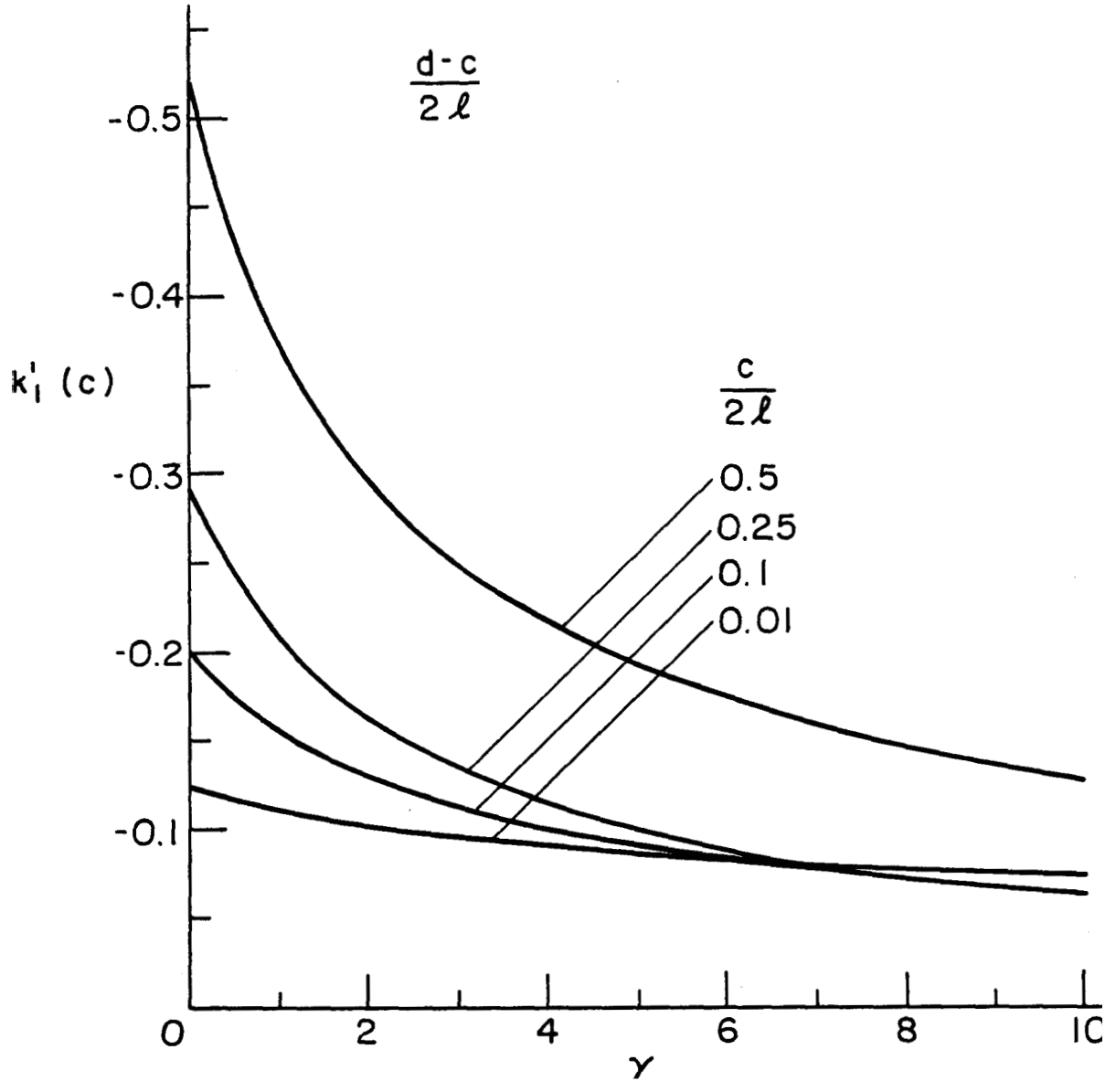

Figure 23. Stress intensity factor at the inclusion end y = c; $\sigma^{\infty}_{YY} \neq 0$, $\sigma^{\infty}_{xx} = \sigma^{\infty}_{xy} = 0$, $\nu = 0.3$, $\theta = \pi/2$, d-c = 2ℓ, b = R = -a.

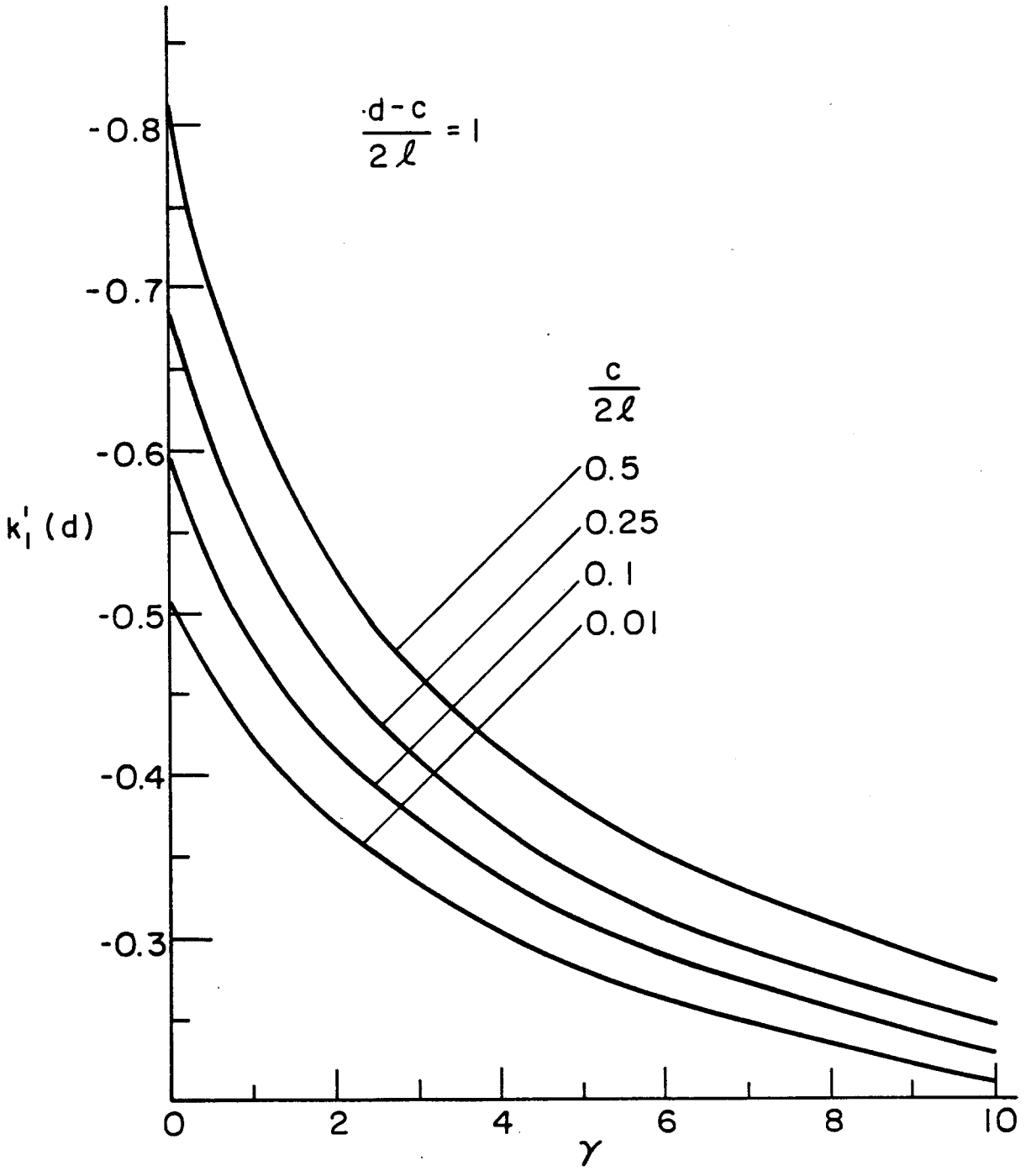

Figure 24. Stress intensity factor at the inclusion end y=d; $\sigma_{yy}^{\infty} \neq 0$, $\sigma_{xx}^{\infty} = \sigma_{xy}^{\infty} = 0$, $\nu = 0.3$, $\theta = \pi/2$, d-c = 2ℓ, b = R = -a.

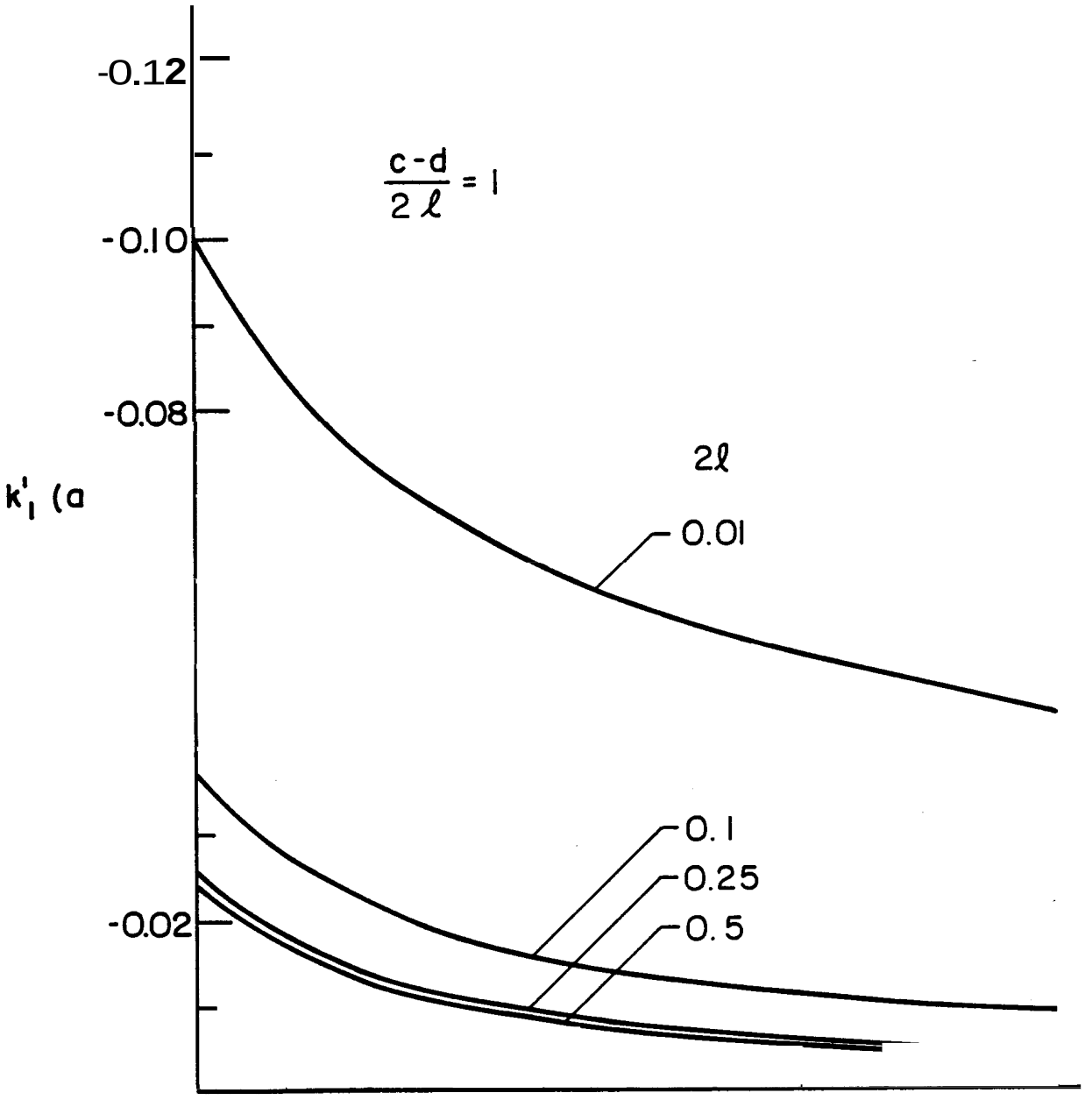

Figure 25. Mode I stress intensity factor at the crack tip $x = a = -\ell$; $\sigma^{\infty}_{xx} \neq 0$, $\sigma^{\infty}_{YY} = \sigma^{\infty}_{xy} = 0$, $\nu = 0.3$, $\theta = \pi/2$, $b = \ell$, $d-c = 2\ell$

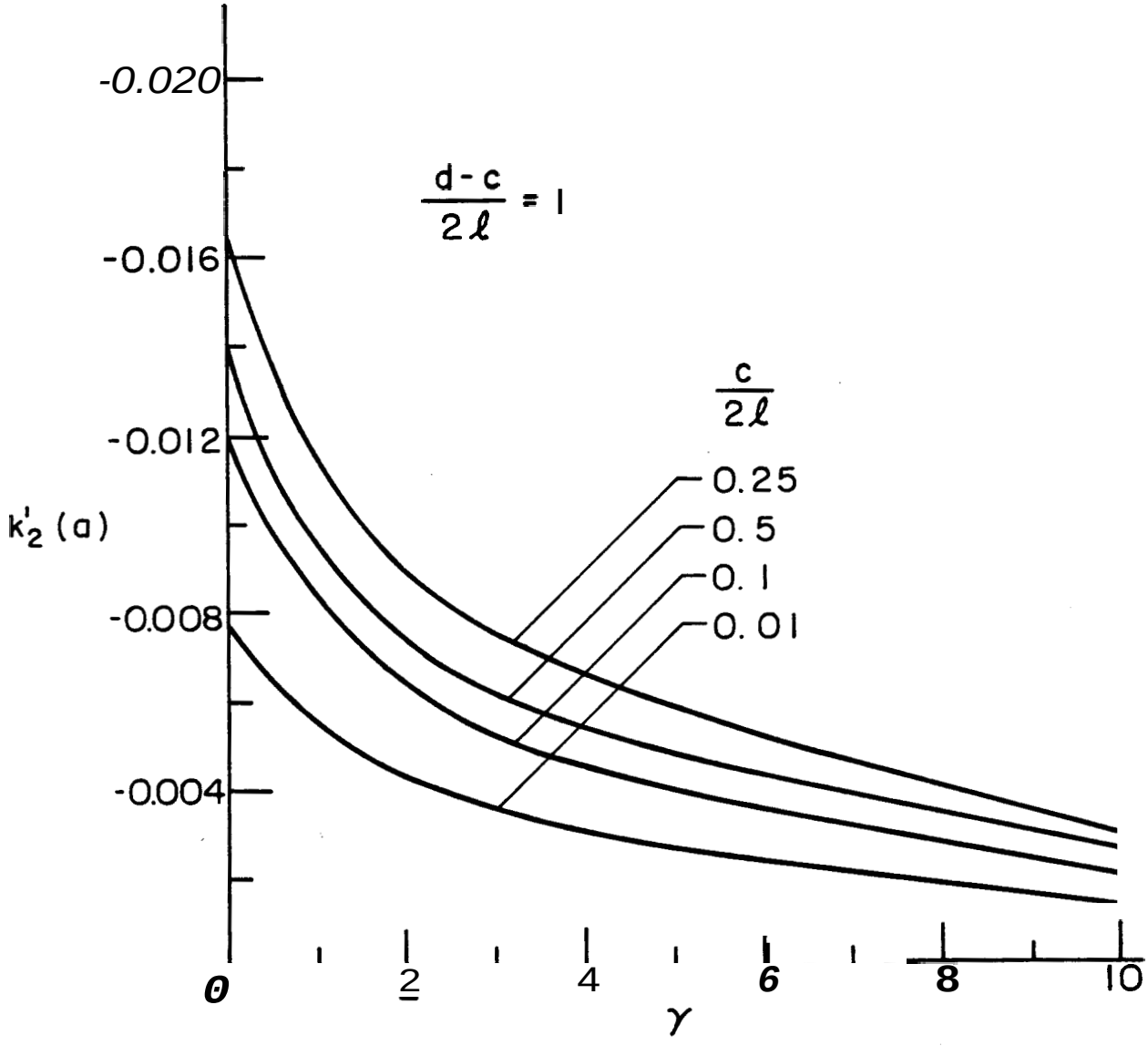

Figure 26. Mode II stress intensity factor at the crack tip $x = a = -\ell$; $\sigma^{\infty}_{xx} \neq 0$, $\sigma^{\infty}_{yy} = \sigma^{\infty}_{xy} = 0$, $\nu = 0.3$, $\theta = \pi/2$, $d-c = 2\ell$, $b = R$.

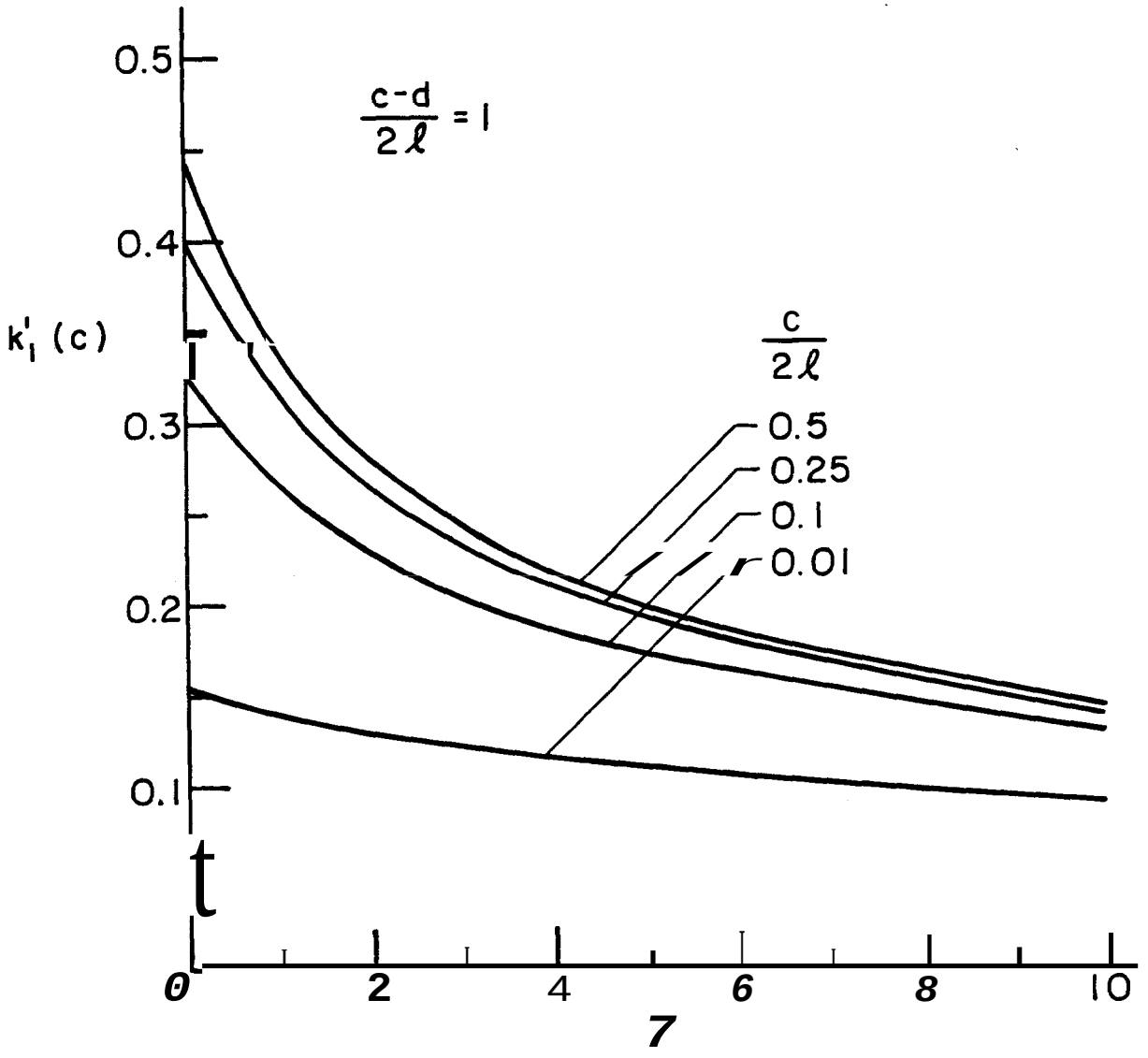

Figure 27. Stress intensity factor at the inclusion end y = c; $\sigma_{xx}^{\infty} \neq 0$, $a_{YY} = \sigma_{xy}^{\infty} = 0$, $\nu = 0.3$, $\theta = \pi/2$, $d-c = 2\ell$, $b = \ell = -a$.

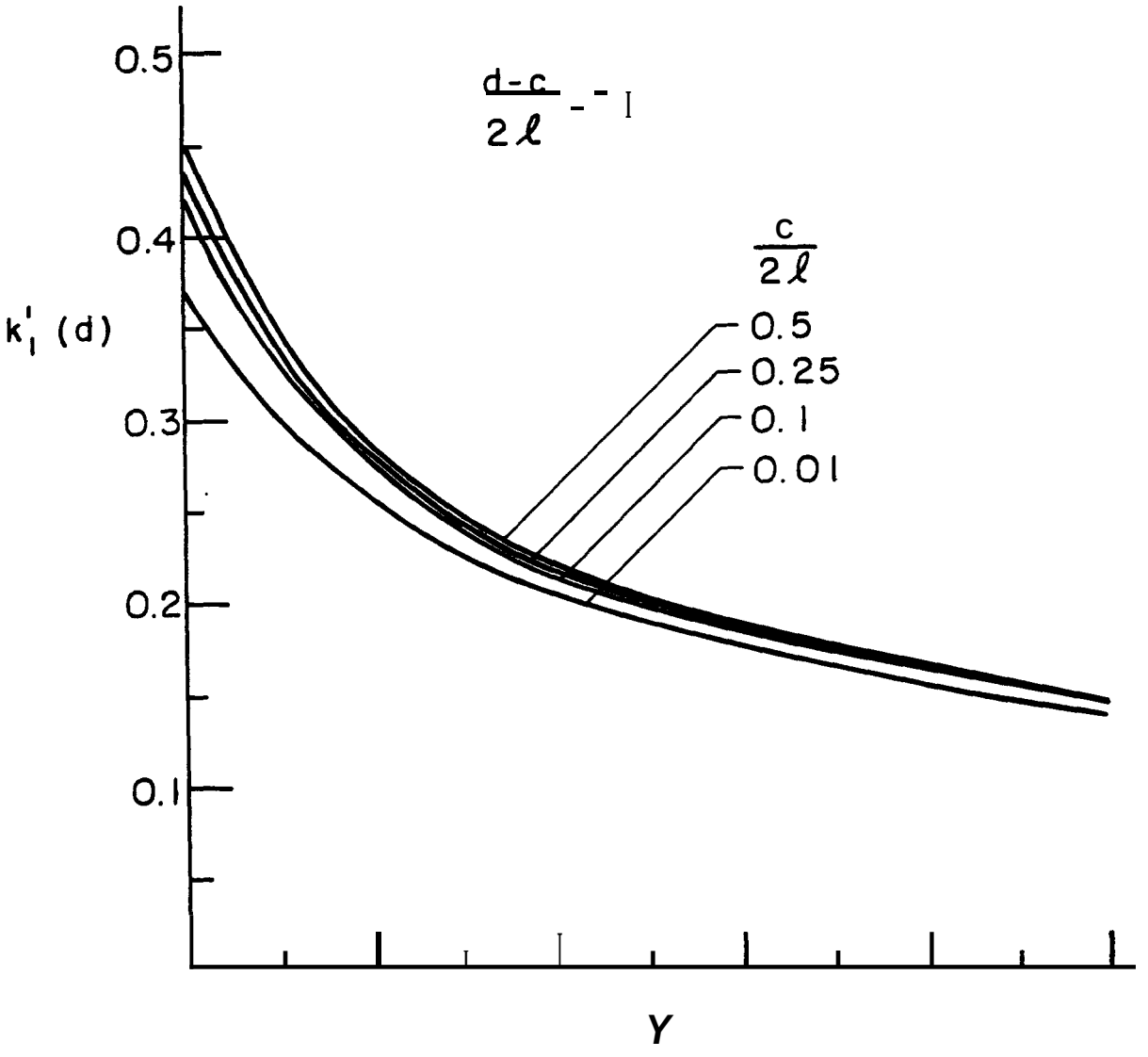

Figure 28. Stress intensity factor at the inclusion end y = d; $\sigma^{\infty}_{XX} \neq 0$, $\sigma^{\infty}_{YY} = \sigma^{\infty}_{xy} = 0$, $\nu = 0.3$, $\theta = \pi/2$, d-c = 2ℓ, b = ℓ = -a.

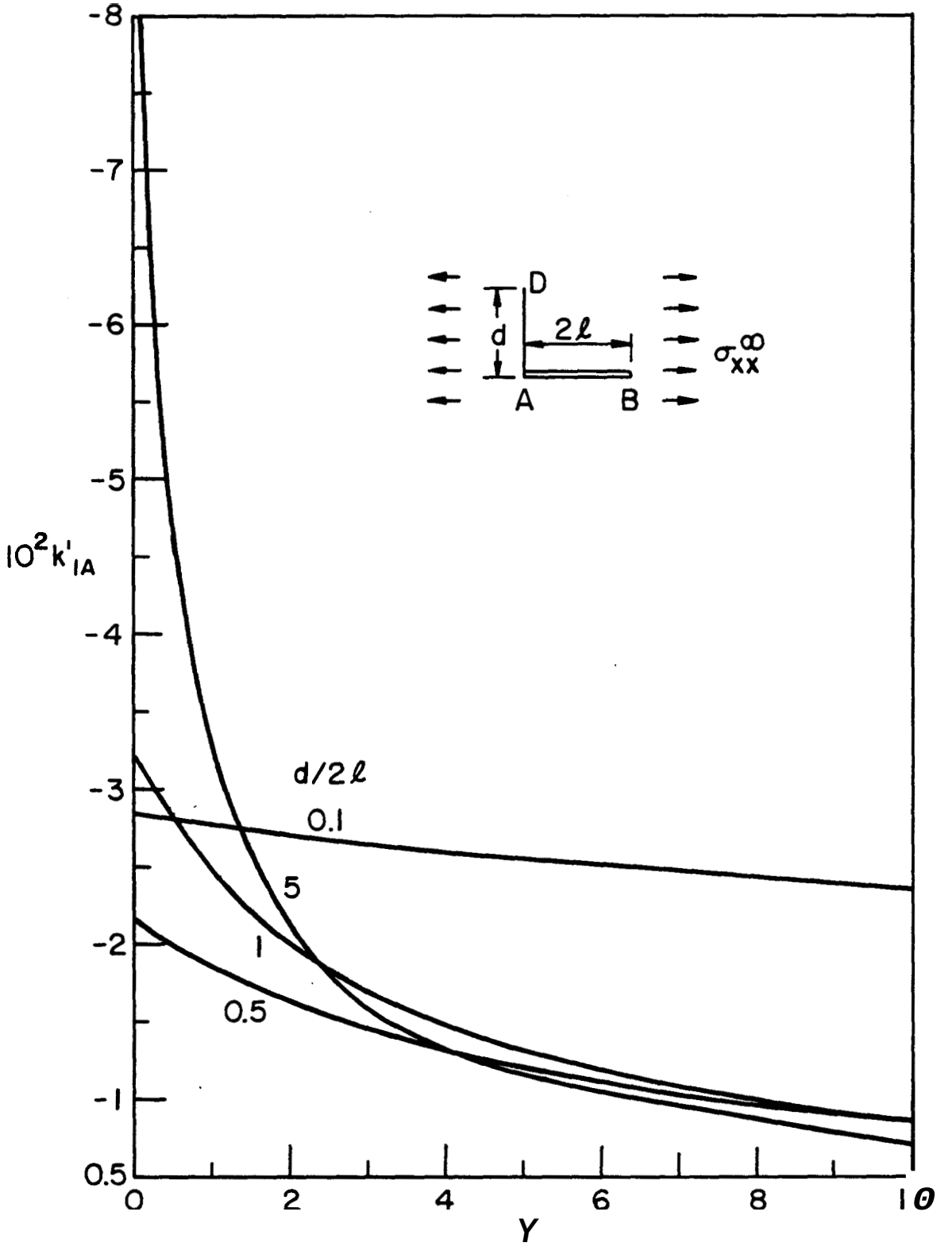

Figure 29. Normalized stress intensity factor for the inclusion-crack intersection problem for which $\theta = \pi/2$, a = 0, b = 2ℓ, c = 0, d/2ℓ and γ variables. k_{1A} for $\sigma_{xx}^{\infty} \neq 0$, $\sigma_{xy}^{\infty} = 0$, $\sigma_{yy}^{w} = 0$.

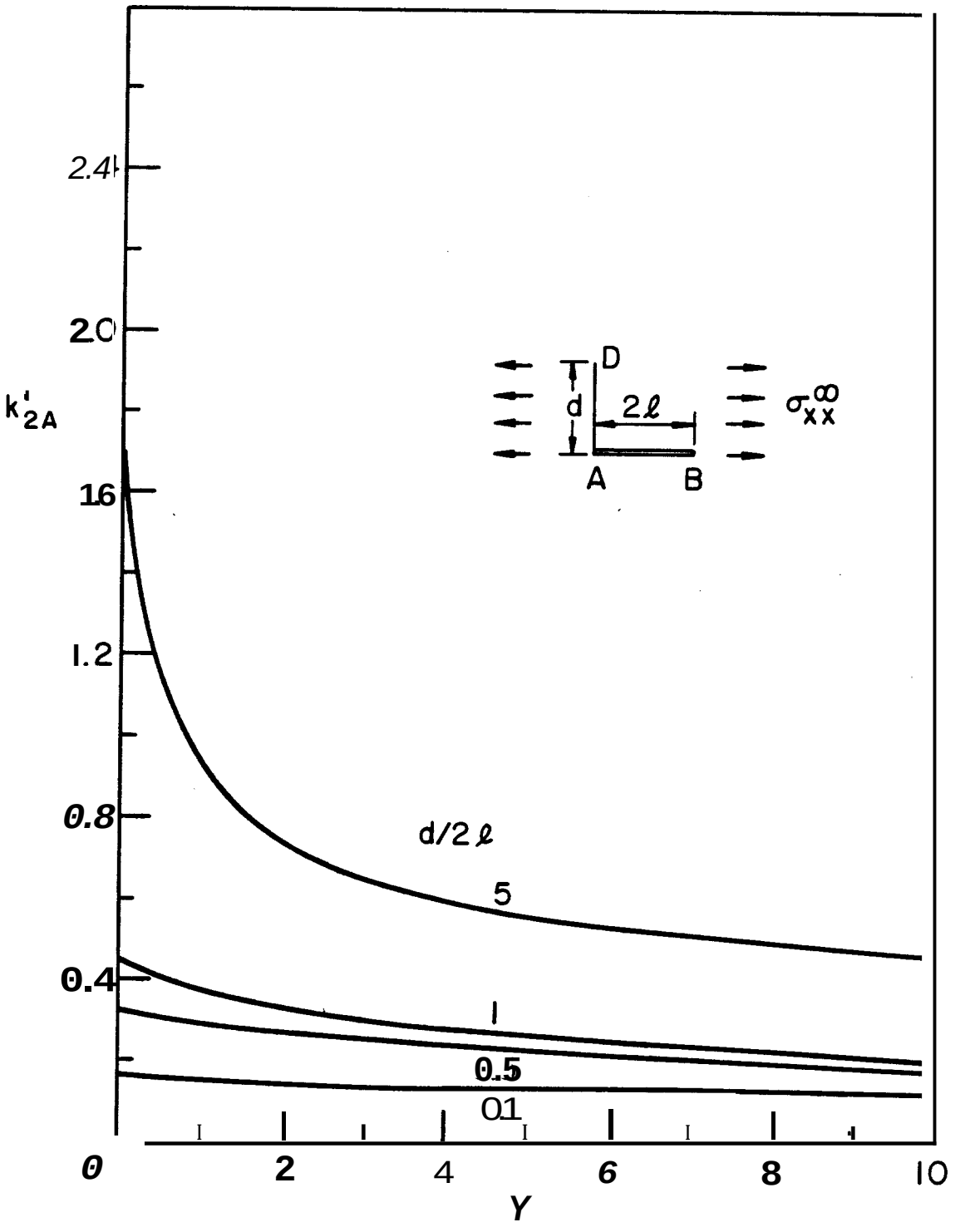

Figure 30. Normalized stress intensity factor for the inclusion-crack intersection problem for which $e = \pi/2$, $a = 0$, $b = 2\ell$, $c = 0$, $d/2\ell$ and γ variables. k'_{2A}, $\sigma^{\infty}_{xx} = 0$, $\sigma^{\infty}_{xy} = \sigma^{\infty}_{YY} = 0$.

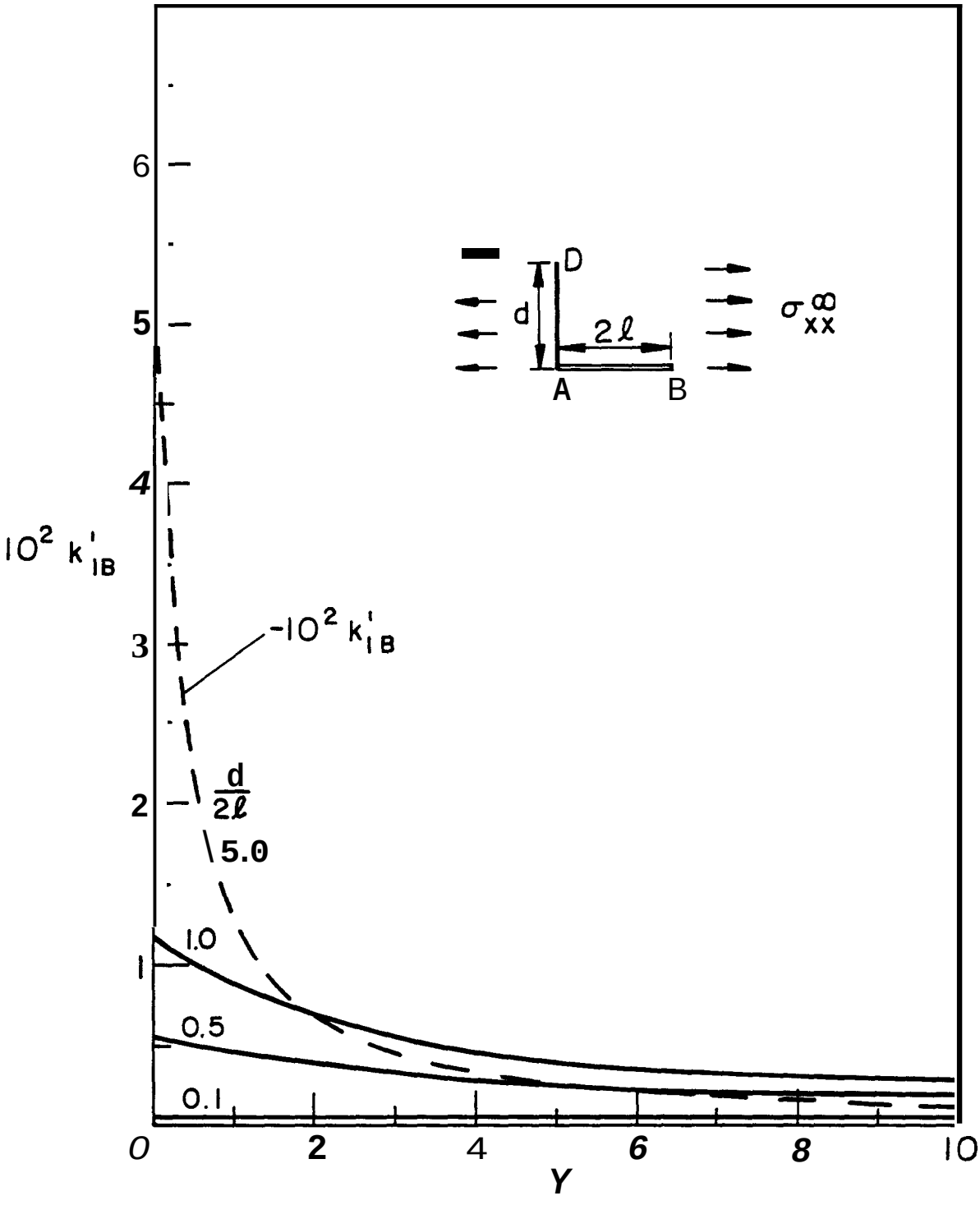

Figure 31. Normalized stress intensity factor for the inclusion-crack intersection problem for which $e = \pi/2$, $a = 0$, $b = 2\ell$, $c = 0$, $d/2\ell$ and γ variables. k'_{IB} , $\sigma^{\infty}_{xx} \neq 0$.

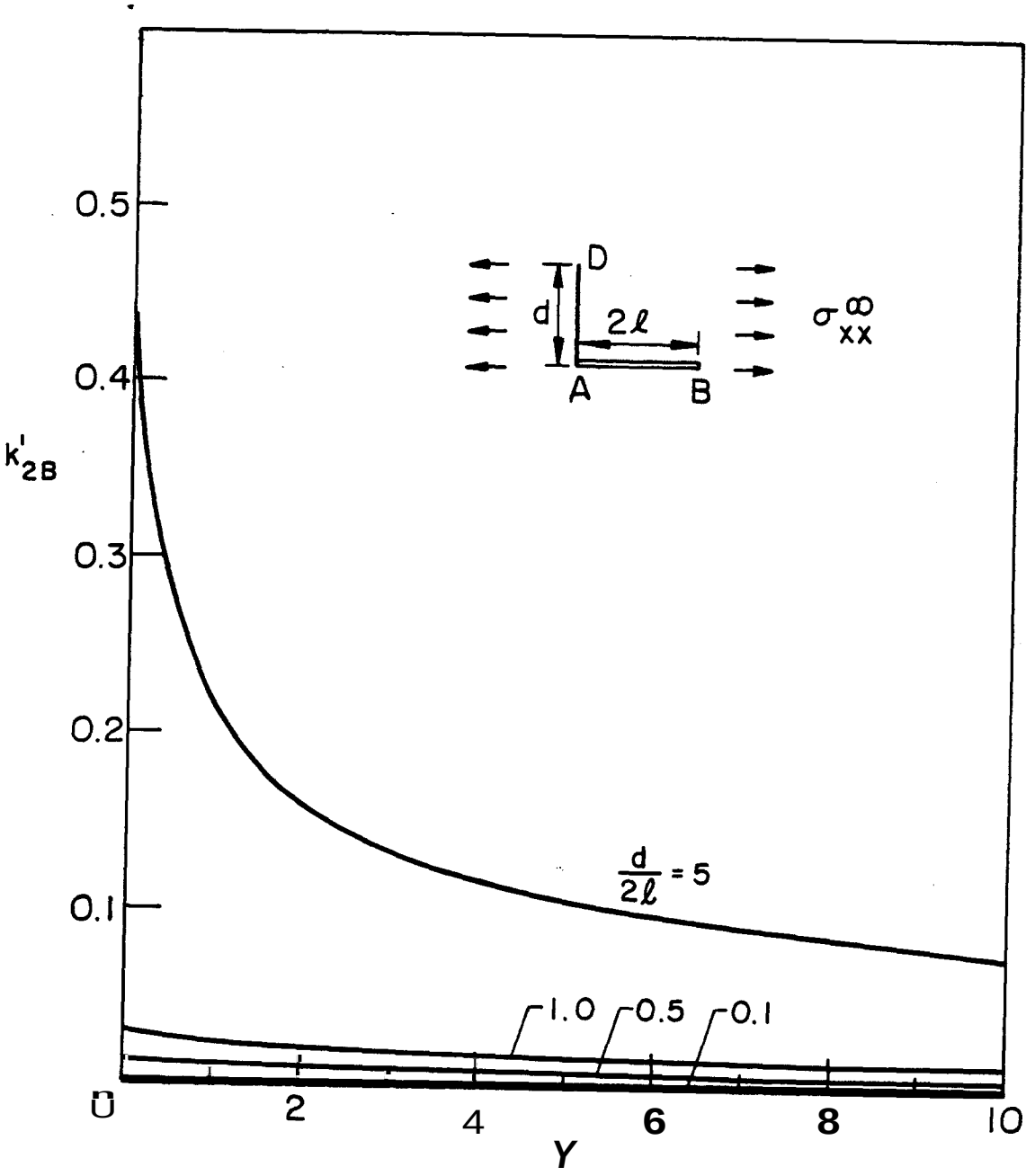

Figure 32. Normalized stress intensity factor for the inclusion-crack intersection problem for which $\theta = \pi/2$, $a = 0$, $b = 2\ell$, $c = 0$, $d/2\ell$ and γ variables. k'_{2B} , $\sigma^{\infty}_{xx} \neq 0$.

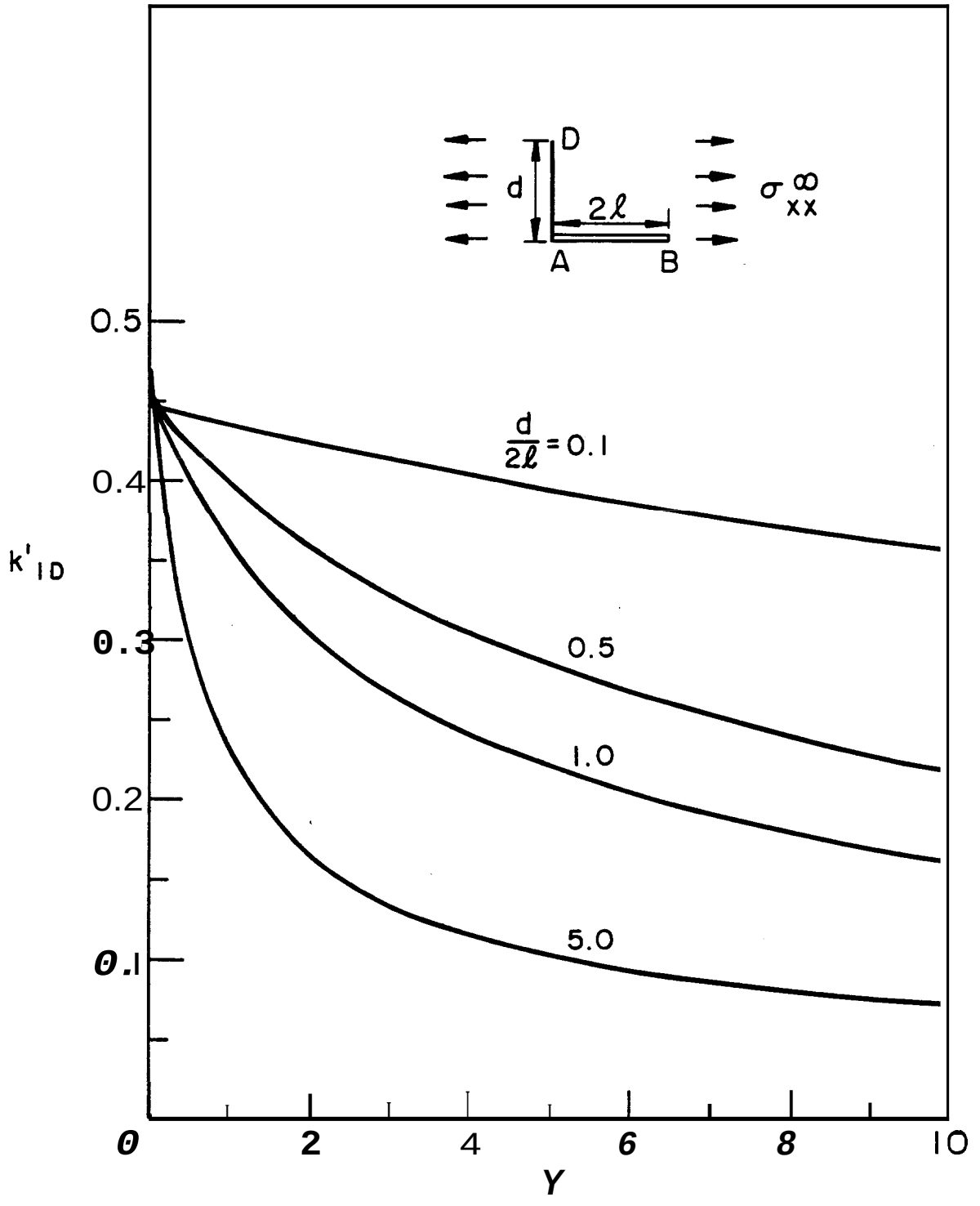

Figure 33. Normalized stress intensity factor for the inclusion–crack intersection problem for which $\theta = \pi/2$, a = 0, b = 2ℓ, c = 0, d/2ℓ and γ variables. k_{1D}, $\sigma^{\infty}_{xx} = 0$.

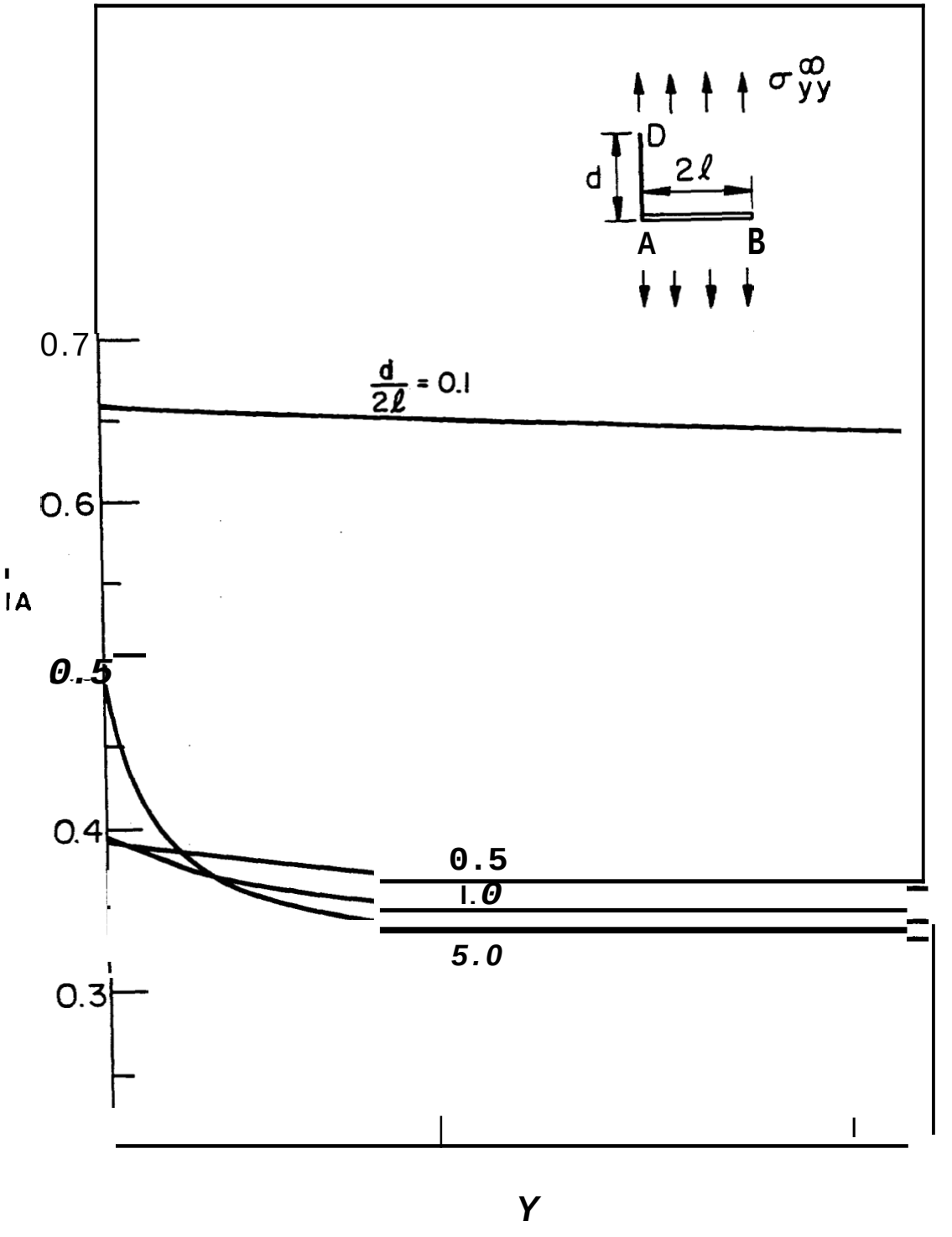

Figure 34. Normalized stress intensity factor for the inclusion-crack intersection problem for which $\theta = \pi/2$, a = 0, b = 2ℓ, c = 0, d/2ℓ and γ variables. $k_{1A}, \sigma^{\infty}_{yy} \neq 0$.

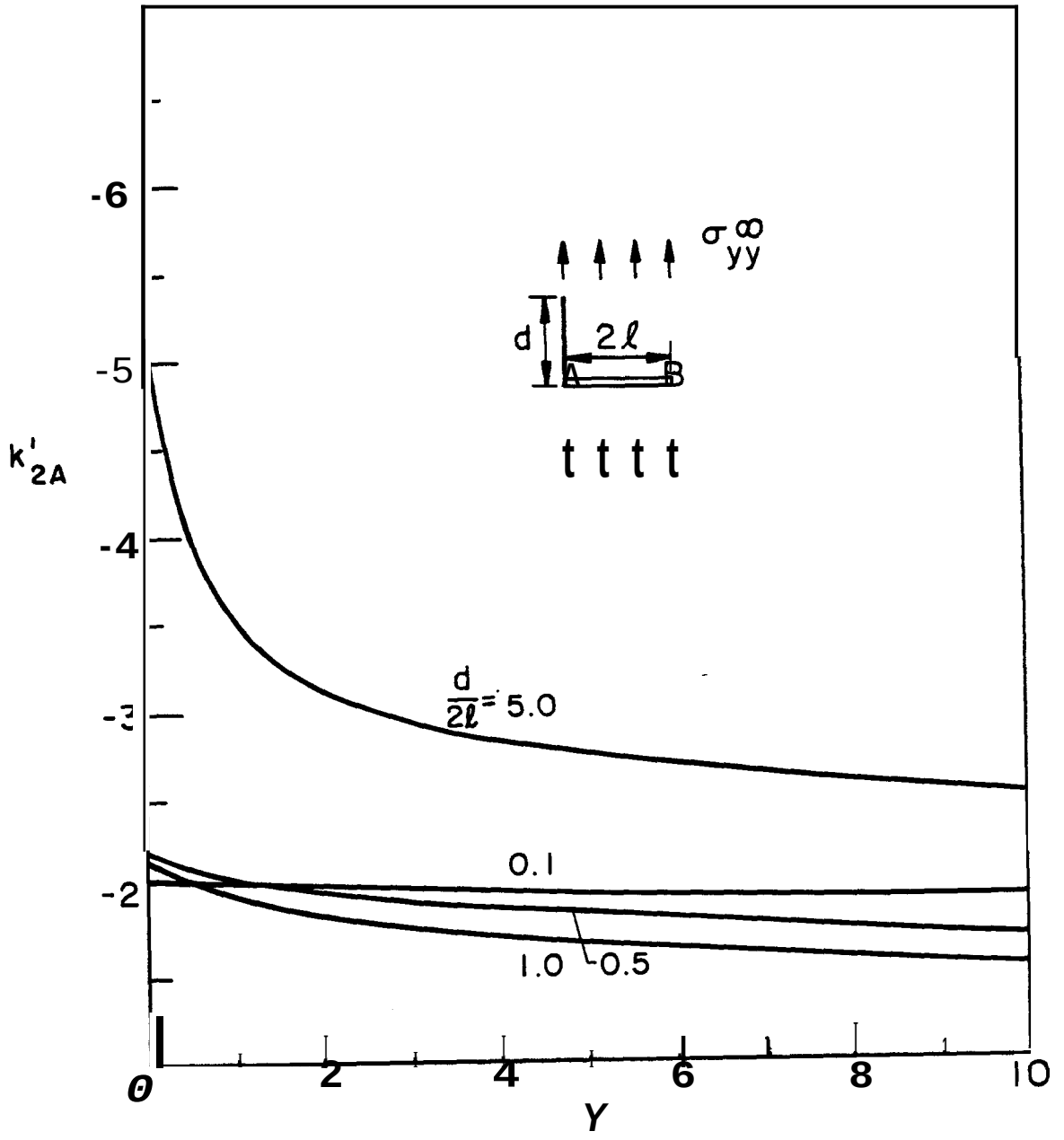

Figure 35. Normalized stress intensity factor for the inclusion-crack intersection problem for which $\theta = \pi/2$, a = 0, b = 2ℓ, c = 0, $d/2\ell$ and γ variables. k_{2A} , $\sigma^{\infty}_{yy} \neq 0$.

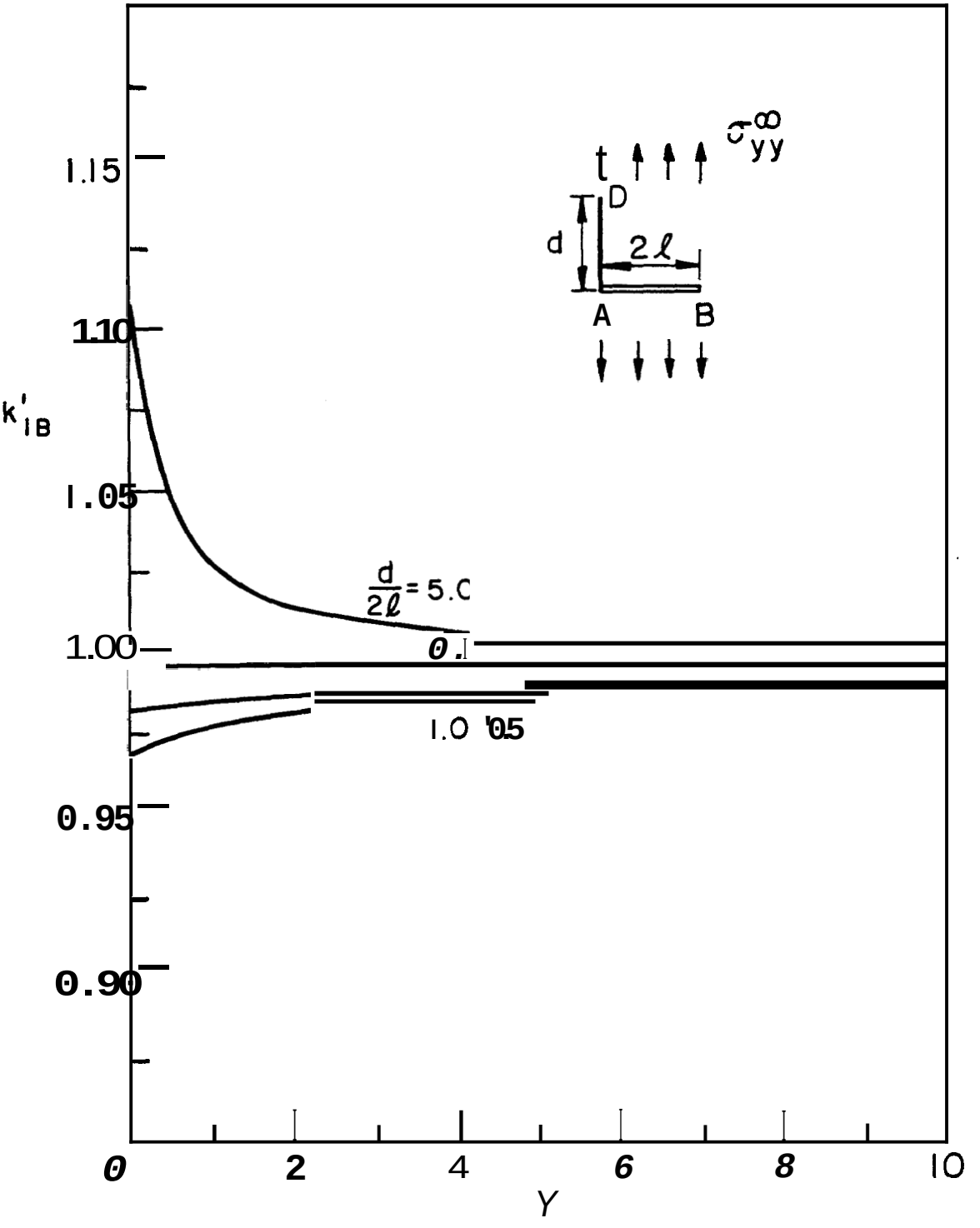

Figure 36. Normalized stress intensity factor for the inclusion–crack intersection problem for which $e = \pi/2$, $a = 0$, $b = 2\ell$, $c = 0$, $d/2\ell$ and γ variables. k'_{IB}, $\sigma^{\infty}_{yy} \neq 0$.

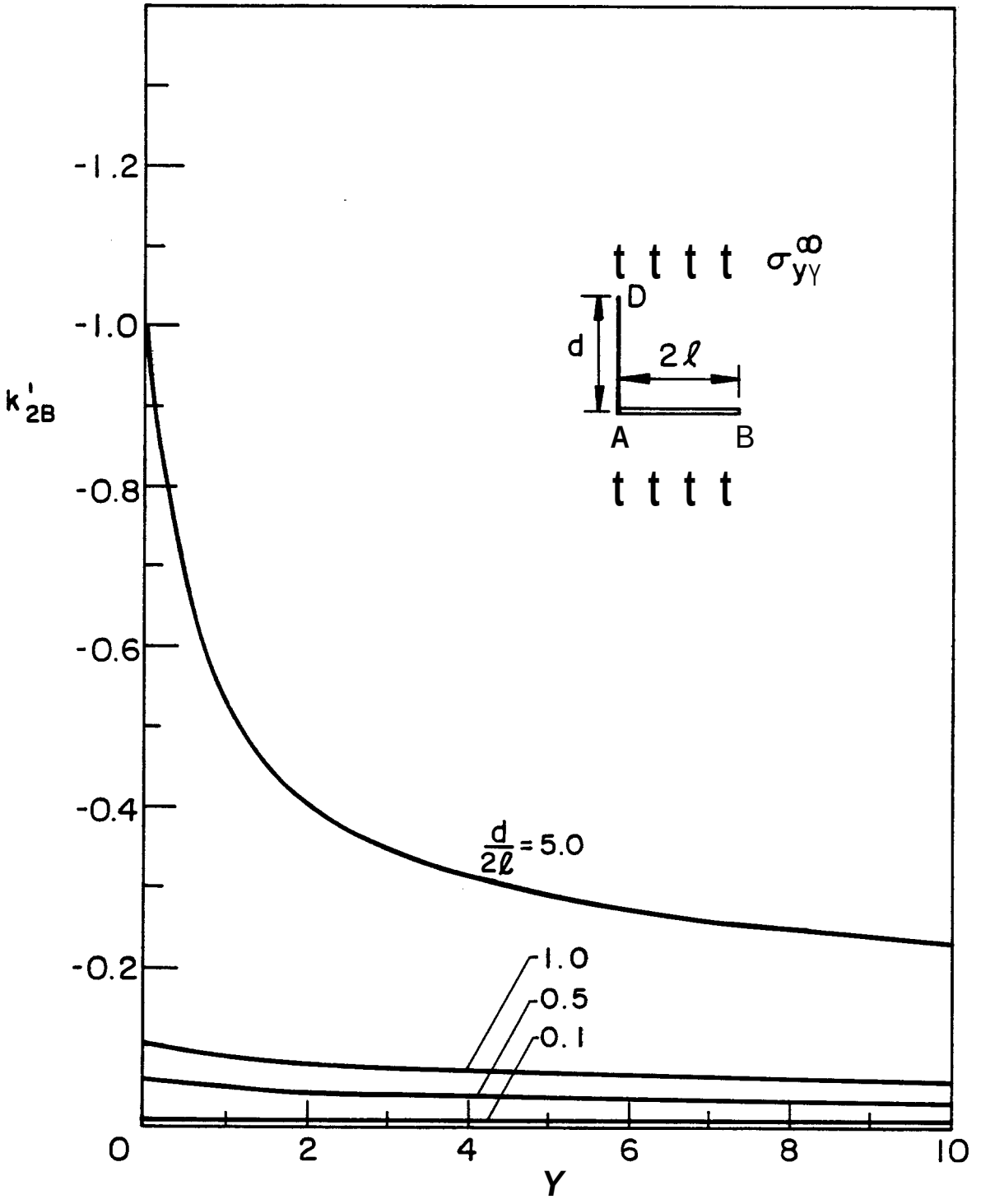

Figure 37. Normalized stress intensity factor for the inclusion-crack intersection problem for which $\theta = \pi/2$, a = 0, b = 2ℓ, c = 0, d/2ℓ and γ variables. k_{2B} , $\sigma^{\infty}_{YY} \neq 0$.

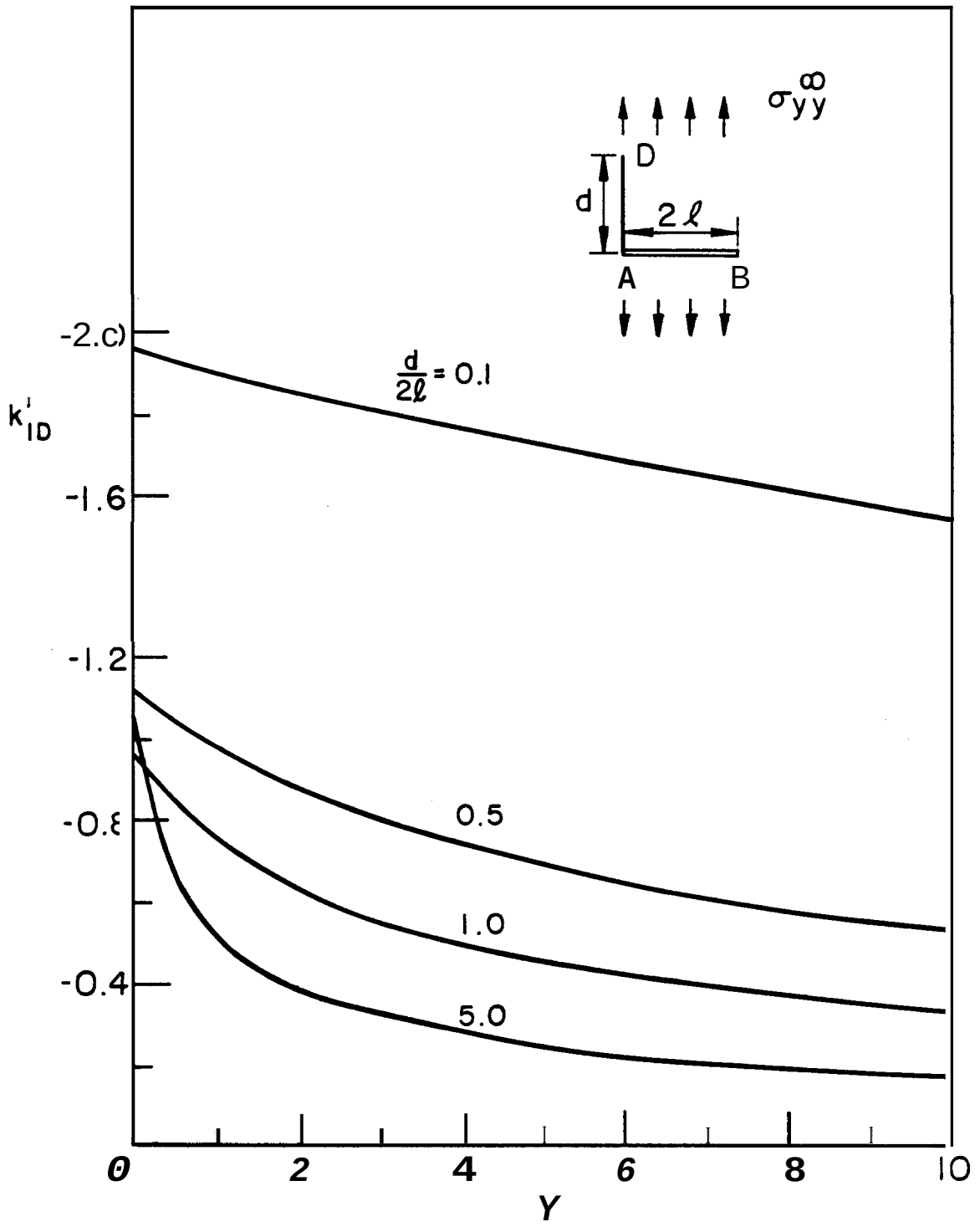

Figure 38. Normalized stress intensity factor for the inclusion-crack intersection problem for which $e = \pi/2$, $a = 0$, $b = 2\ell$, $c = 0$, $d/2\ell$ and γ variables. k_{1D}, $\sigma_{YY}^{\infty} \neq 0$.

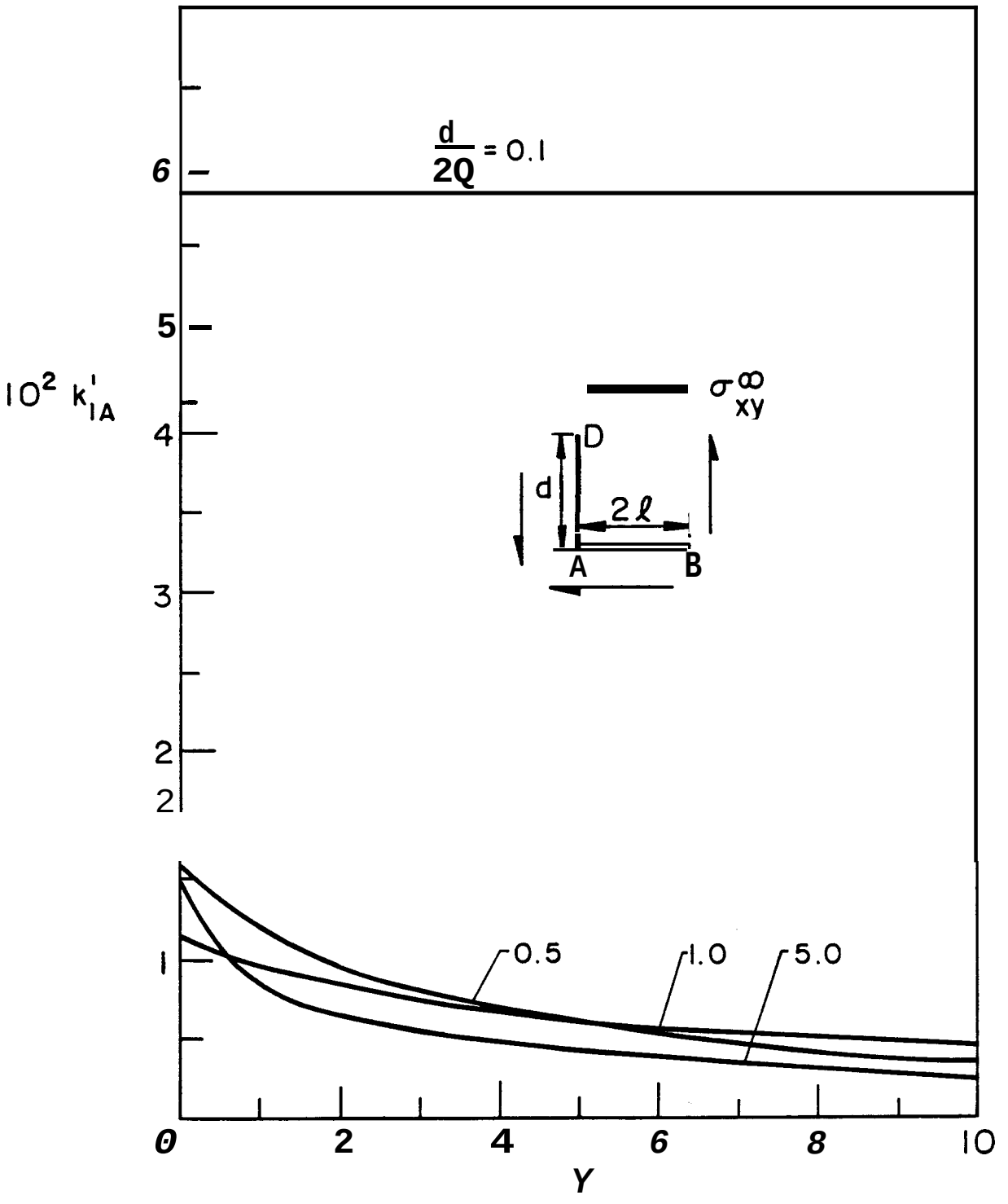

Figure 39. Normalized stress intensity factor for the inclusion-crack intersection problem for which $e = \pi/2$, $a = 0$, $b = 2\ell$, $c = 0$, $d/2\ell$ and γ variables. k_{IA} , $\sigma^{\infty}_{xy} \neq 0$.

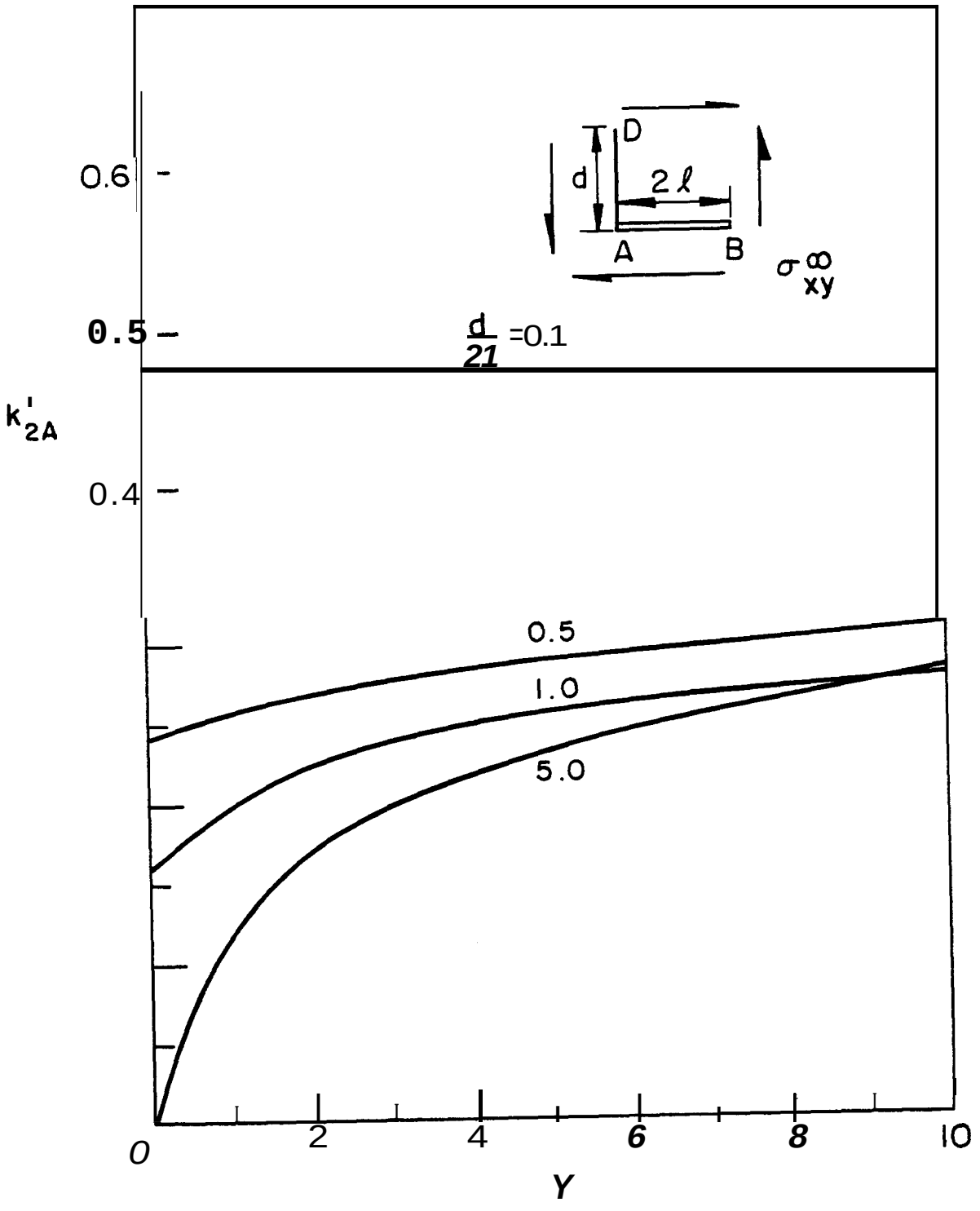

Figure 40. Normalized stress intensity factor for the inclusion-crack intersection problem for which $e = \pi/2$, $a = 0$, $b = 2\ell$, $c = 0$, $d/2\ell$ and γ variables. k_{2A} , $\sigma^{\infty}_{xy} \neq 0$.

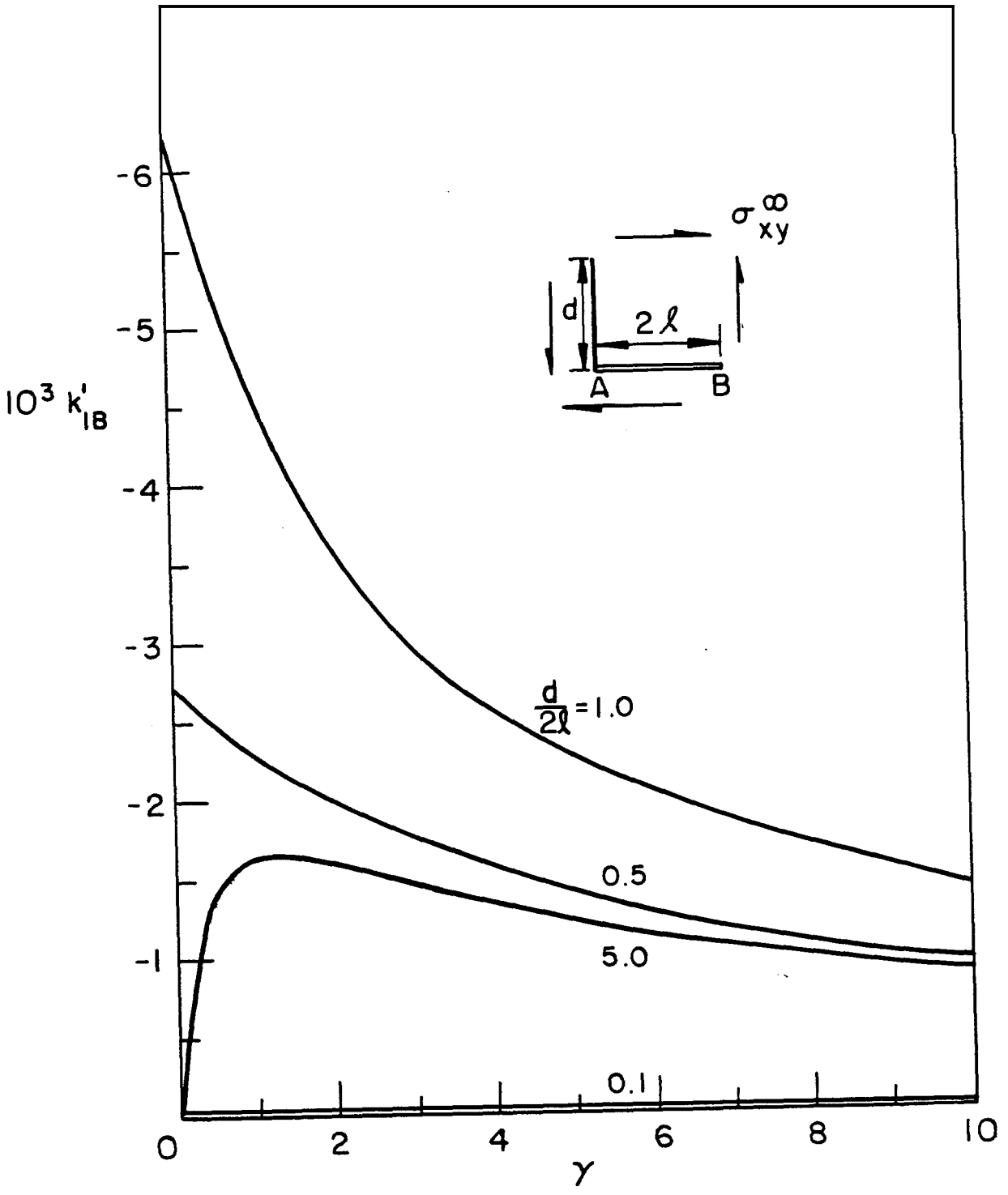

Figure 41. Normalized stress intensity factor for the inclusion-crack intersection problem for which $e = \pi/2$, $a = 0$, $b = 2\ell$, $c = 0$, $d/2\ell$ and γ variables. k_{1B} , $\sigma^{\infty}_{xy} \neq 0$.

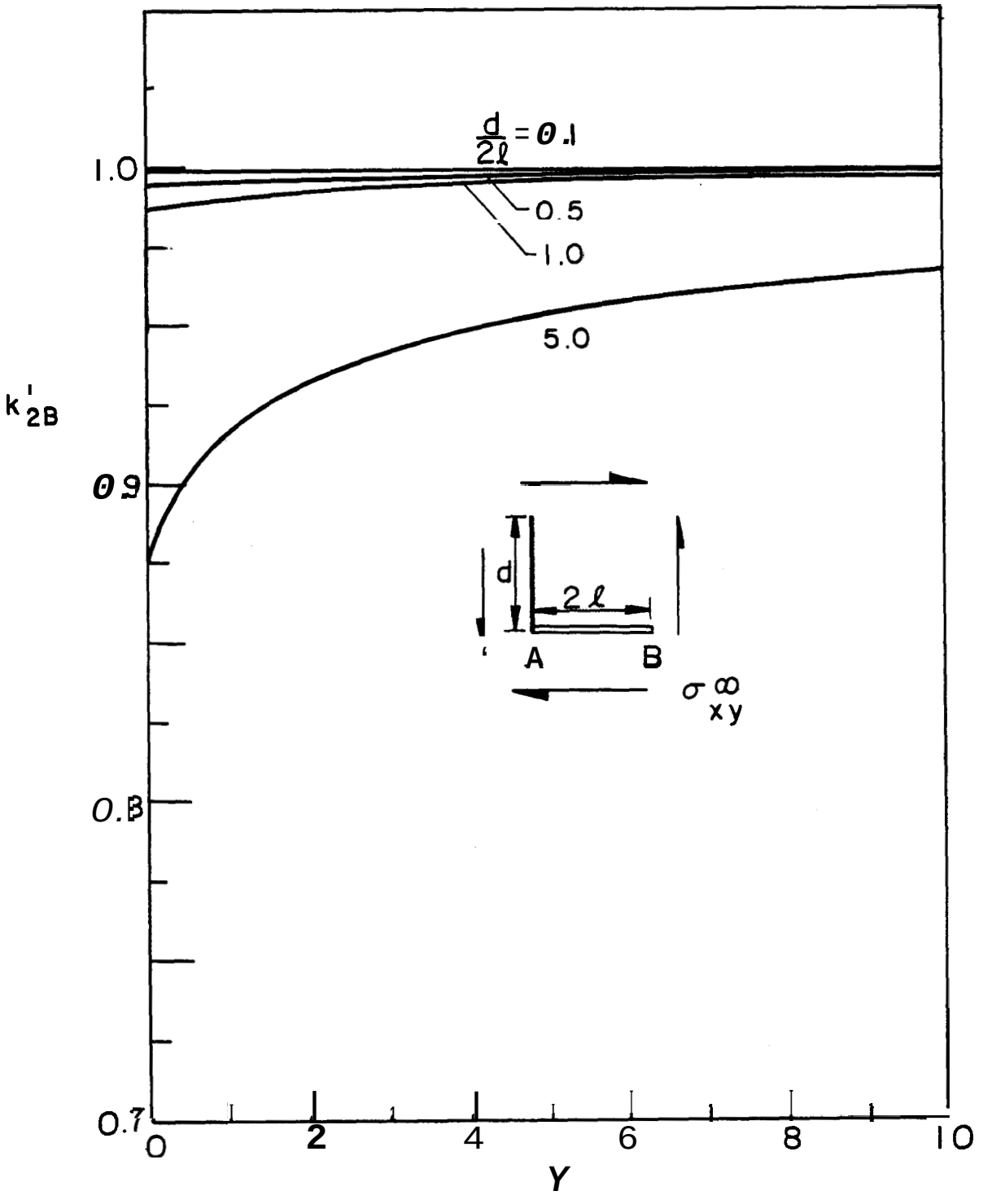

Figure 42. Normalized stress intensity factor for the inclusion-crack intersection problem for which $\theta = \pi/2$, $a = 0$, $b = 2\ell$, $c = 0$, $d/2\ell$ and γ variables. k_{2B} , $\sigma_{xy} \neq 0$.

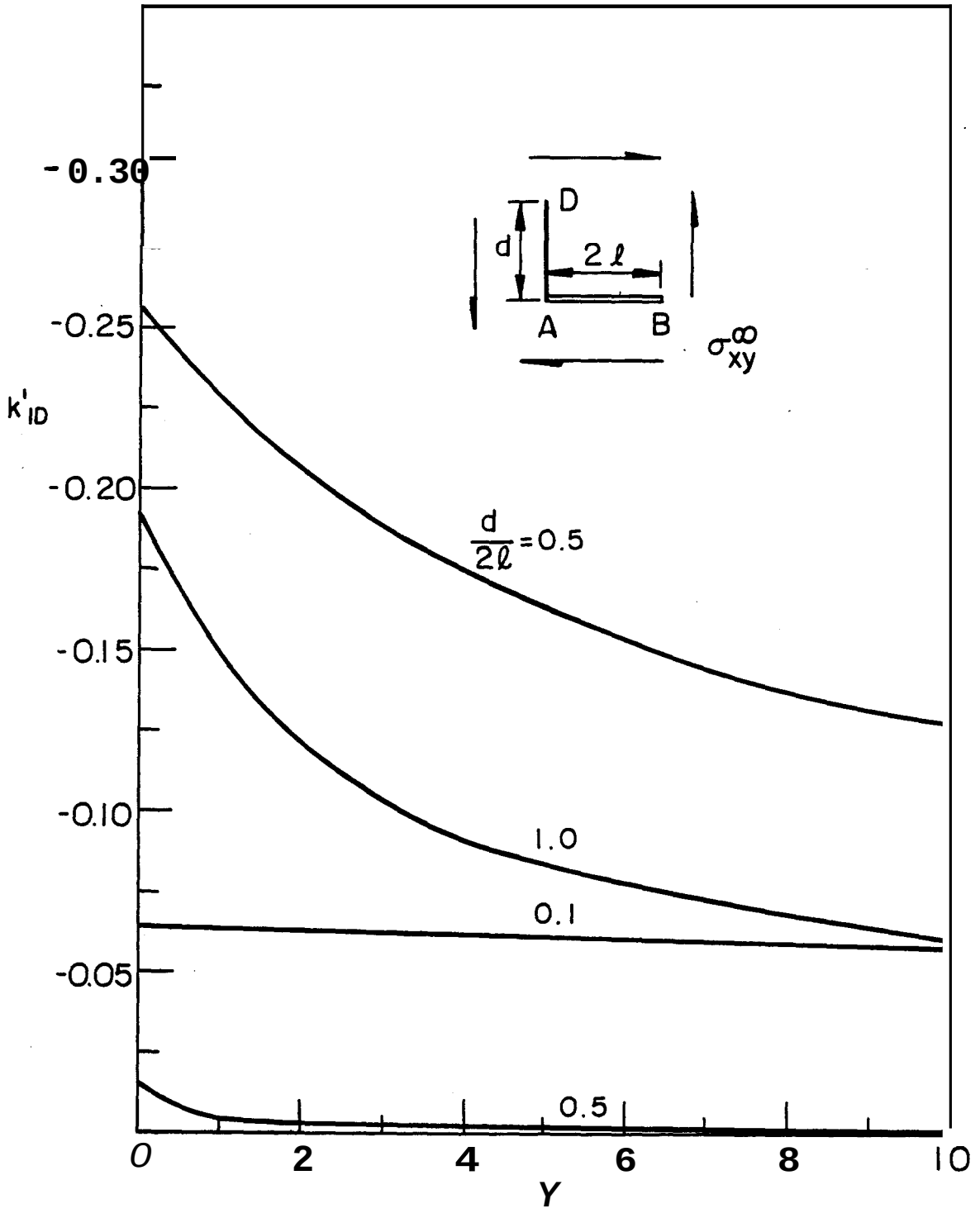

Figure 43. Normalized stress intensity factor for the inclusion-crack intersection problem for which $\theta = \pi/2$, a = **0**, **b** = 2ℓ, c = 0, $d/2\ell$ and γ variables. k'_{1D} , $\sigma^{\infty}_{xy} \neq 0$.